

**A more detailed and quantitative
consideration of organized
convection: Part III**

Supercell thunderstorms

Miller Composite Sounding Types

Some background from Bluestein's book

U.S. Air force began forecasting based on upper-air observations in 1948 in response to a tornado hitting Tinker Air Force base near Oklahoma City

1952 The Severe Local Storms Forecasting unit of the Weather Bureau started to forecast severe weather

SELS moved to Kansas City and become National Severe Storms Forecasting Center in 1966. Later moved to Norman, Oklahoma

Four characteristics soundings associated with strong convection identified, developed by Col. R. Miller (in Air Force Manual)

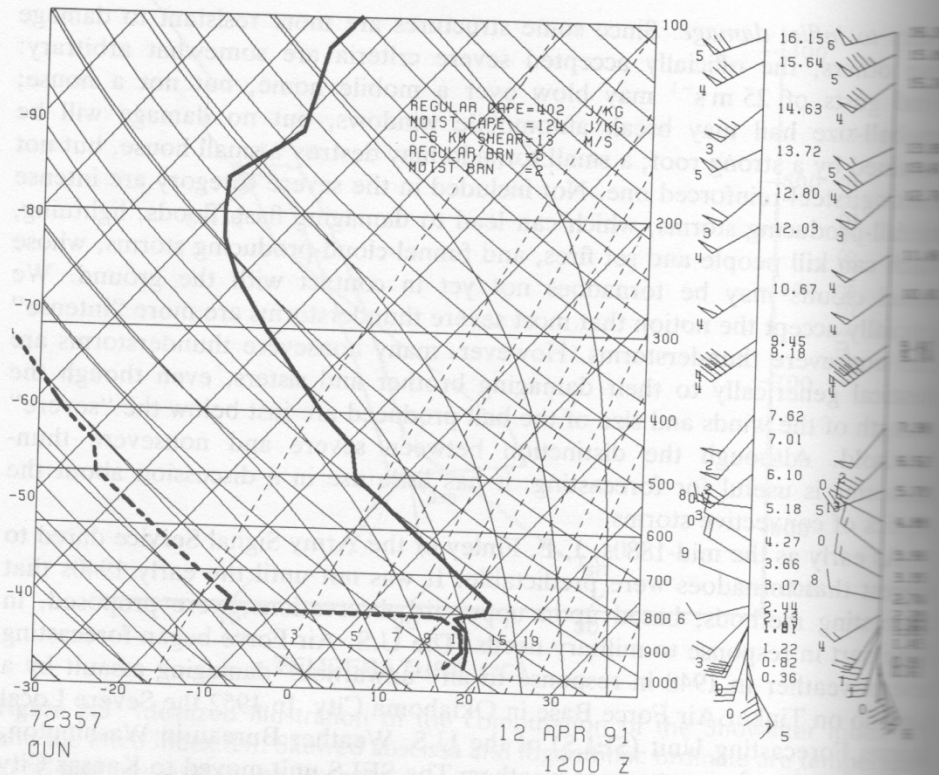


Figure 3.10 Example of a typical Miller “Type I” sounding in the United States. Sounding is at Norman, Oklahoma, at 1200 UTC, April 12, 1991 (0600 LST). Skewed abscissa and logarithmic ordinate are temperature ($^{\circ}\text{C}$) and pressure (mb), respectively. The plot of temperature and dew point are given by the thick solid and dashed lines, respectively. Winds plotted at the right; pennant = 25 m s^{-1} ; whole barb = 5 m s^{-1} ; half barb = 2.5 m s^{-1} . The moist air in the boundary layer (surface to 810 mb) comes from the Gulf of Mexico; the mixing ratio from the surface to 850 mb is nearly constant. The layer of low static stability above the moist layer comes from an elevated, deep, dry boundary layer over Mexico. The air above the Mexican layer (above 450 mb) comes from the western United States. The latter is separated from the former by a 50-mb deep stable layer. A stable layer, which in this case is an inversion, caps the moist layer around 800 mb. Several tornadic thunderstorms occurred in north-central Oklahoma later on in the day.

MILLER TYPE I

Well mixed, moist boundary layer of about 100-mb. High theta-e air.

Stable, dry inversion above low-level moist layer (cap)

Cold and very unstable aloft.

Directional shear.

The “loaded gun” sounding discussed earlier in reference to supercell thunderstorms

MILLER TYPE II

The tropical sounding

Deep moist layer up to at least seven km, so pretty close to moist adiabatic.

Little if any capping inversion

Possibility of widespread convection, but typically not too severe

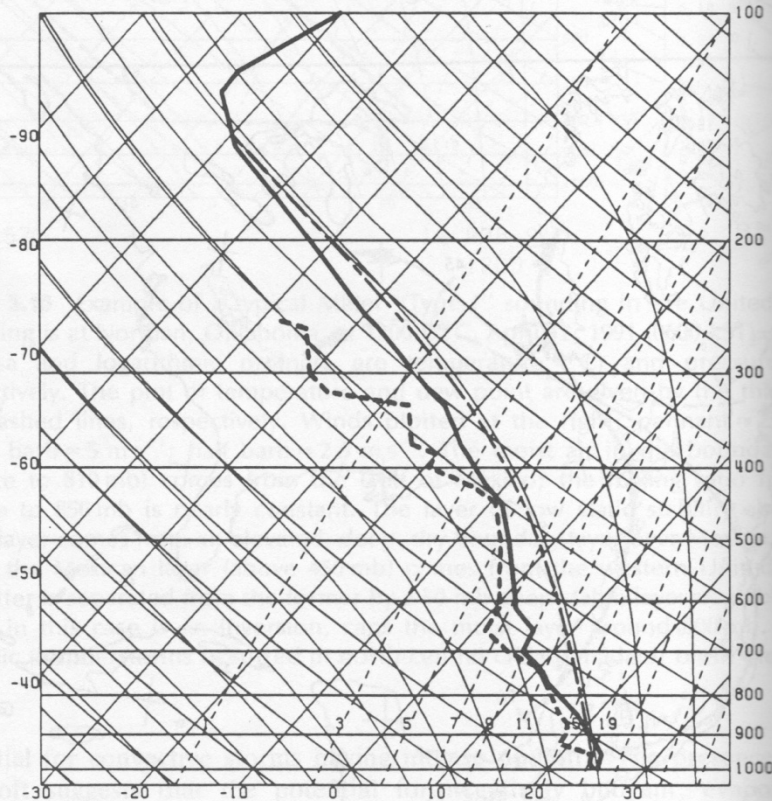


Figure 3.12 Example of a Miller "Type II" sounding in the United States. Skewed abscissa and logarithmic ordinate are temperature ($^{\circ}\text{C}$) and pressure (mb). Temperature (solid line); dew point (dashed line); moist-adiabat along which surface air parcel ascends (dot-dashed line). For Centerville, Alabama, 0000 UTC, August 17, 1985. This sounding was associated with a tornado outbreak and the remains of Hurricane Danny (from McCaul, 1987). (Courtesy of the American Meteorological Society)

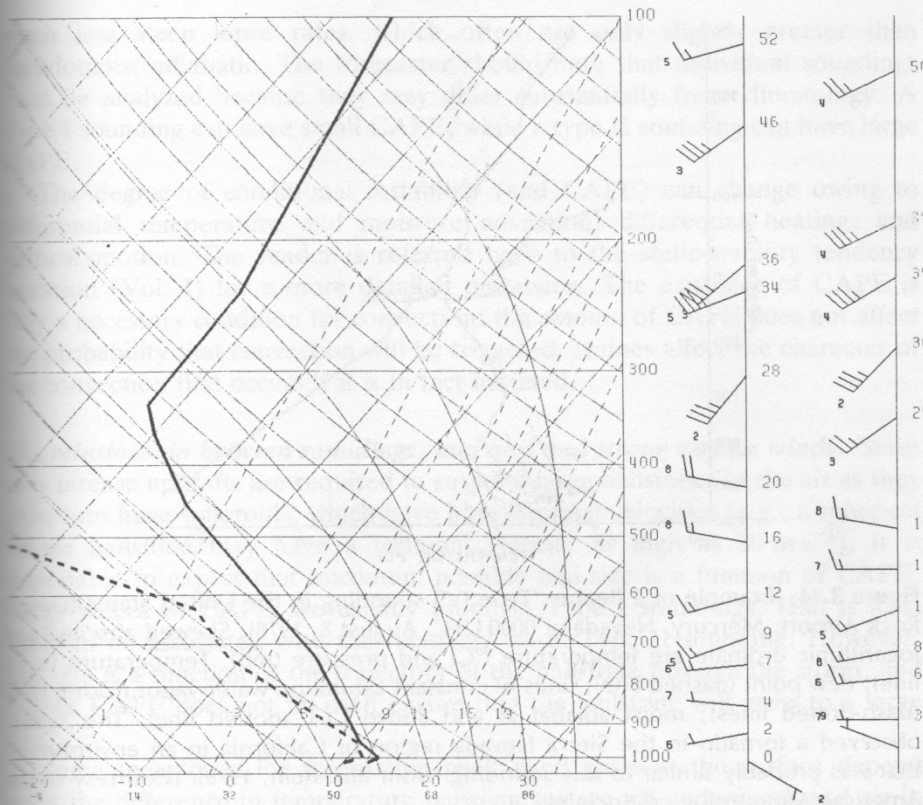


Figure 3.13 Example of a Miller “Type III” sounding in the United States. Sounding for Oakland, California, 1200 UTC, September 10, 1985. Skewed abscissa and logarithmic ordinate are temperature (°C) and pressure (mb), respectively. The plot of temperature and dew point are given by the thick solid and dashed lines, respectively. Winds plotted at the right; whole barb = 5 m s^{-1} ; half barb = 2.5 m s^{-1} . A waterspout was reported over nearby San Francisco Bay near the time of this sounding. A cold upper-level low was situated over Northern California. Note the relatively cold -25°C temperature at 500 mb, and the relatively low tropopause (about 325 mb); also note the weak vertical wind shear and light land breeze at the surface from the southeast.

MILLER TYPE III

Similar to type II, except much colder (by 10-15 degrees C)

Found in cold core of upper-level cyclones and troughs.

“Cold air” sounding

MILLER TYPE IV

No low-level moist layer.

Relative humidity increase with height in lower troposphere

High surface temperature with a deep, well mixed boundary layer that is nearly dry adiabatic.

The “inverted V” profile .

Produced when dry continental tropical air overlaid by cold, moist polar air.

Sounding for microbursts!

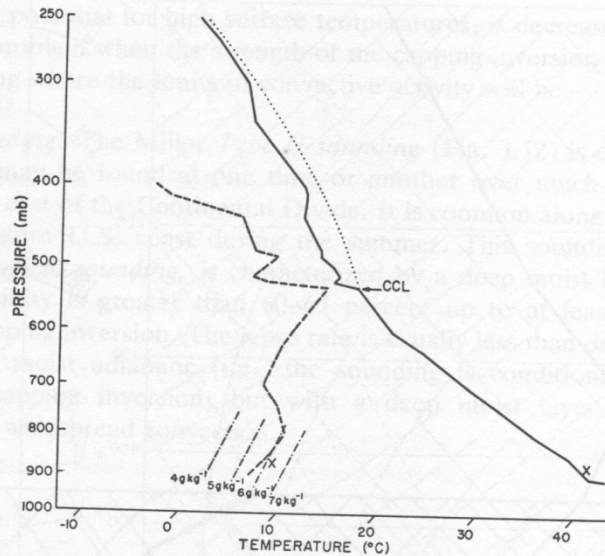


Figure 3.14 Example of a Beebe “Type IV” sounding in the United States (Desert Rock Airport, Mercury, Nevada at 0000 UTC, August 8, 1978). Skewed abscissa and logarithmic ordinate are temperature ($^{\circ}\text{C}$) and pressure (mb). Temperature (solid line); dew point (dashed line); lines of constant saturation water-vapor mixing ratio (dash-dotted lines); moist adiabat at and above CCL (dotted line). The author observed a tornado in the Sierra Nevada region of California in an environment that was probably similar to this sounding (from Bluestein, 1979). (Courtesy of the American Meteorological Society)

Development of mid-level rotation for mesocyclone.

How do we get a fast rotating mesocyclone.
updraft, with relatively large vertical
vorticity (ζ)?

→ Have to have some way to

- 1) tilt horizontal vorticity into vertical
→ source
- 2) stretch the vorticity in vertical
→ increase the spin.

Recall from our previous derivation of the
vertical vorticity equation, we obtained
tendency equations for horizontal and
vertical components

Tendency equation for vertical vorticity (ζ),
omitting planetary rotation:

$$\frac{\partial \zeta}{\partial t} = \underbrace{-\vec{v} \cdot \nabla \zeta}_{(1)} + \underbrace{\vec{\omega} \cdot \nabla \omega}_{(2)}$$

$$\vec{\omega} = (\xi, \eta, \zeta) \quad \begin{array}{l} \text{Total} \\ \text{vorticity} \\ \text{vector} \end{array}$$

- (1) Advection term
- (2) Vortex stretching / tilting term.

Expanding!

$$\frac{\partial \zeta}{\partial t} = -u \frac{\partial \zeta}{\partial x} - v \frac{\partial \zeta}{\partial y} - w \frac{\partial \zeta}{\partial z} \\ + \xi \frac{\partial \omega}{\partial x} + \eta \frac{\partial \omega}{\partial y} + \zeta \frac{\partial \omega}{\partial z}$$

Explicitly writing out the horizontal
vorticity components!

$$\frac{\partial \zeta}{\partial t} = -u \frac{\partial \zeta}{\partial x} - v \frac{\partial \zeta}{\partial y} - w \frac{\partial \zeta}{\partial z}$$

Advection

$$+ \left(\frac{\partial \omega}{\partial y} - \frac{\partial v}{\partial z} \right) \frac{\partial \omega}{\partial x} + \left(\frac{\partial u}{\partial z} - \frac{\partial \omega}{\partial x} \right) \frac{\partial \omega}{\partial y}$$

Tilting of horizontal
vorticity into vertical.

$$+ \left(\frac{\partial v}{\partial x} - \frac{\partial u}{\partial y} \right) \frac{\partial \omega}{\partial z}$$

Stretching of vertical
vorticity

Neglect!

- Planetary rotational effects
- Baroclinic vorticity generation in vertical, as result of Boussinesq approx.

Linearize around a mean synoptic base state

$$\begin{aligned} u &= \bar{u}(z) + u' & \text{where } \bar{u}(z) \text{ and} \\ v &= \bar{v}(z) + v' & \bar{v}(z) \text{ would be} \\ w &= w' & \text{taken from a} \\ \zeta &= \zeta' & \text{sounding.} \end{aligned}$$

Neglecting products of perturbations

$$\frac{\partial \zeta'}{\partial t} = \underbrace{-\bar{u} \frac{\partial \zeta'}{\partial x} - \bar{v} \frac{\partial \zeta'}{\partial y}}_{\text{Advection terms}} + \underbrace{\frac{\partial \bar{u}}{\partial z} \frac{\partial w'}{\partial y} - \frac{\partial \bar{v}}{\partial z} \frac{\partial w'}{\partial x}}_{\text{Tilting terms}}$$

Note that stretching term vanishes because stretching is a non-linear effect! We'll come back to it later, though.

Using vector notation

$$\frac{\partial \zeta'}{\partial t} = -\vec{V} \cdot \nabla_h \zeta' + \vec{S} \times \nabla_h w' \cdot \hat{k}$$

$$\vec{V} = \bar{u} \hat{i} + \bar{v} \hat{j}$$

$$\vec{S} = \frac{\partial \vec{V}}{\partial z} \quad \text{Mean vertical wind shear.}$$

In a storm-relative frame with storm velocity \vec{c}

$$\frac{\partial \zeta'}{\partial t} = \underbrace{-\underbrace{(\vec{V} - \vec{c}) \cdot \nabla_h \zeta'}_{\text{Advection}}}_{\text{Advection}} + \underbrace{\vec{S} \times \nabla_h w' \cdot \hat{k}}_{\text{Tilting}}$$

Linear effects
Tilting: Rotate horizontal vorticity into vertical

Advection: Shifts the ζ' field horizontally

Non-linear effects
Stretching: As updraft intensifies, vortex stretching further tightens ζ and strength of updraft.

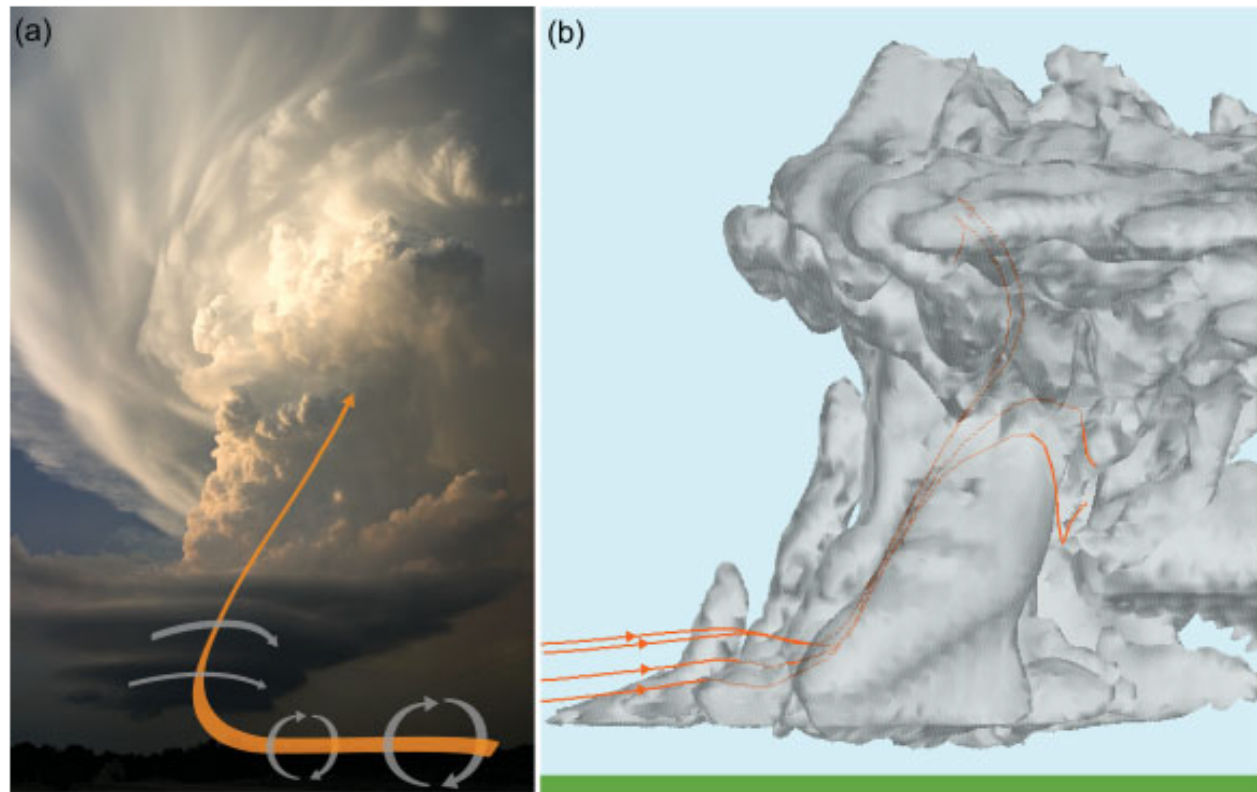
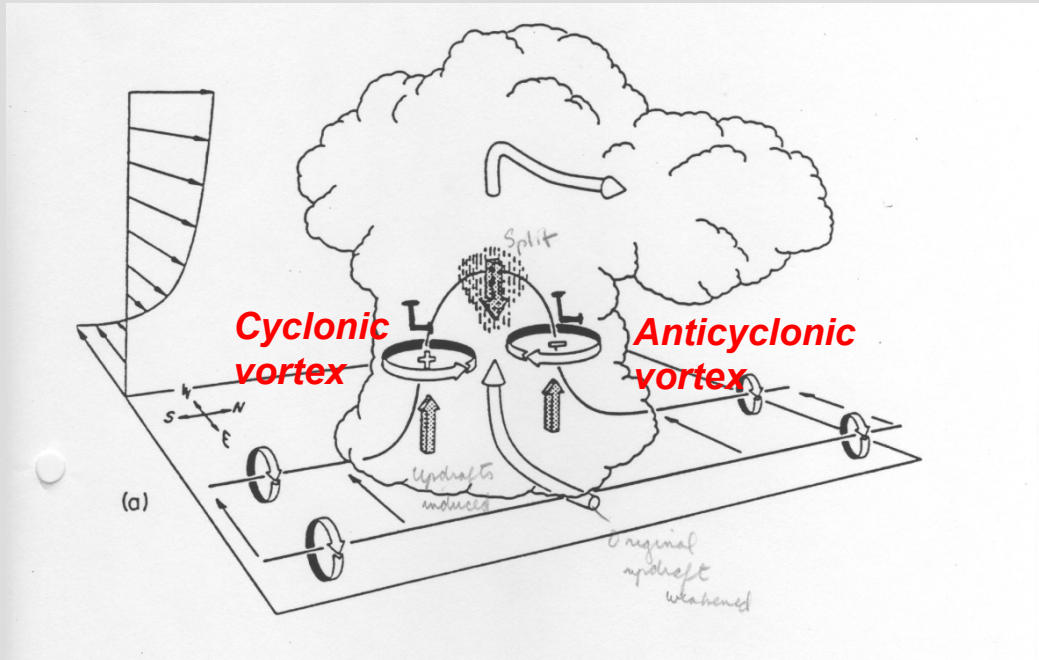
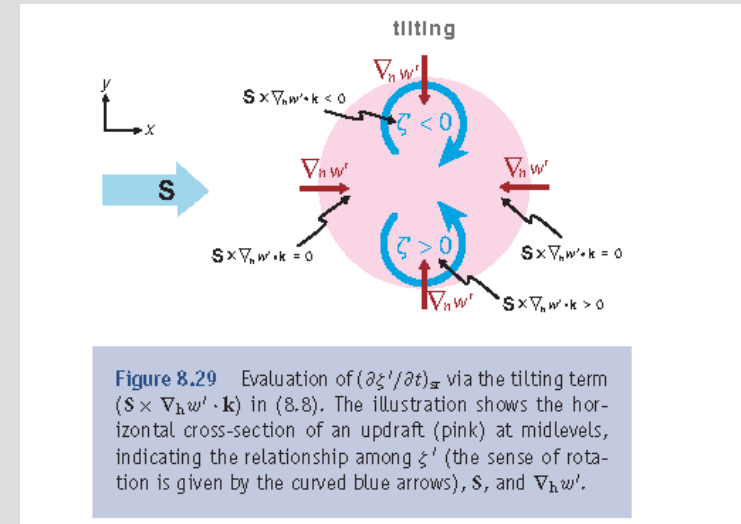


Figure 8.27 Vertical vorticity is acquired by supercells via tilting of horizontal vorticity associated with the vertical shear of the environmental wind profile. (a) Photograph of a supercell updraft. A schematic vortex line has been overlaid. The striated, laminar appearance in the lower portion of the updraft is a visual manifestation of negatively buoyant air being forcibly lifted by a strong, upward-directed, dynamic perturbation pressure gradient force. Such forces arise when buoyant convection develops in environments containing significant vertical wind shear (Section 8.4.5). Photograph courtesy of Eric Nguyen. (b) Numerically simulated supercell updraft (the gray isosurface is the cloud boundary) with actual vortex lines drawn. The vortex lines originate in the low-level inflow and pass through the midlevel mesocyclone. (The model output was displayed using the Vis5D visualization software.)

Downshear side view



Top down view

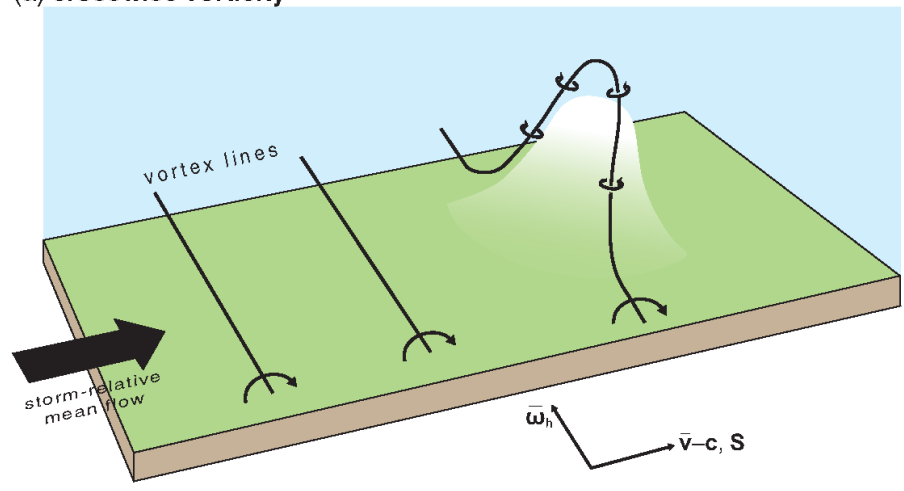


Vorticity couplet straddles the location
of maximum updraft, looking downshear.

$\zeta' > 0$ Cyclonic, right side

$\zeta' < 0$ Anticyclonic, left side

(a) crosswise vorticity



(b) streamwise vorticity

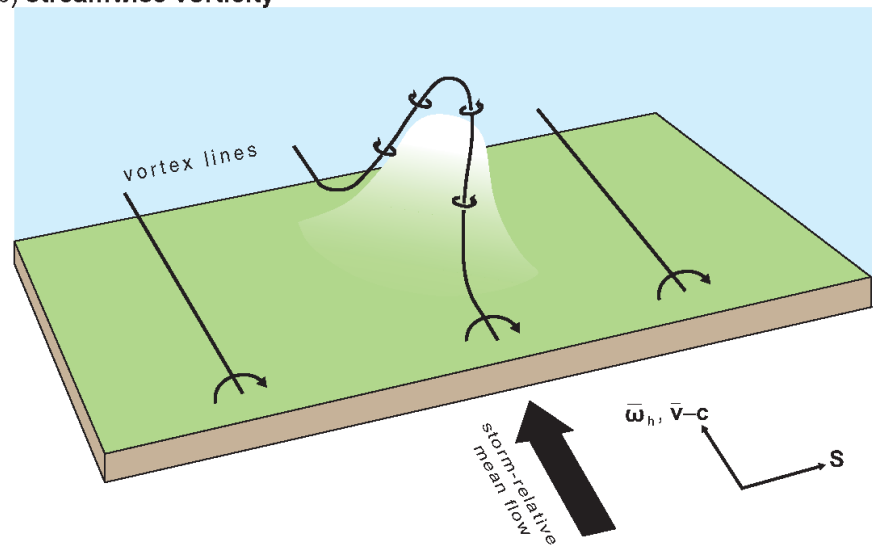


Figure 8.32 Tilting of environmental horizontal vorticity along a hill of constant entropy produces vertical vorticity, whereas storm-relative flow leads to positive (negative) vertical motion on the uphill (downhill) side of the isentropic hill and growth of the hill contributes to positive vertical motion everywhere on the hill. The correlation between w' and ζ' depends on the orientation of the horizontal vorticity $\bar{\omega}_h$ relative to the storm-relative mean wind, $\bar{v}-c$. (a) Tilting of purely crosswise vorticity by an isentropic hill leads to a vortex couplet with zero correlation between w' and ζ' . (b) Tilting of purely streamwise vorticity by an isentropic hill leads to a correlation between w' and ζ' of nearly unity. (Adapted from Davies-Jones [1984].)

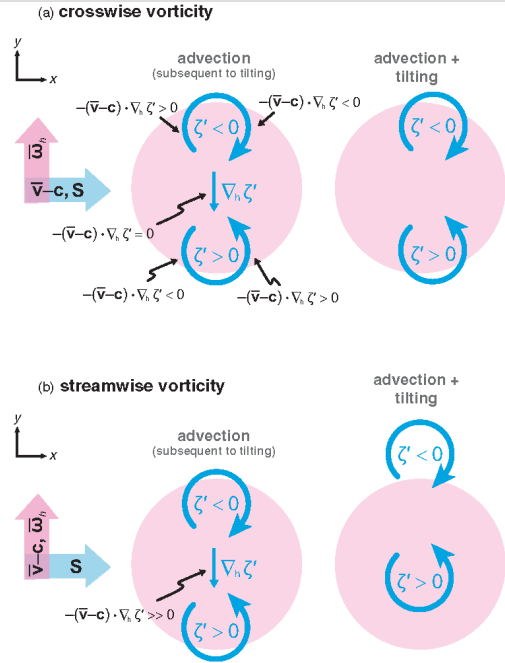


Figure 8.30 Evaluation of $(\partial \zeta' / \partial t)_{st}$ via the advection term $(-\bar{v} - c) \cdot \nabla_h \zeta'$ in (8.8), based on the fact that the tilting term leads to a couplet of vertical vorticity straddling the updraft and oriented normal to the shear vector (cf. Figure 8.29), for the cases of (a) crosswise vorticity and (b) streamwise vorticity. The relationship between the vertical vorticity and vertical velocity fields resulting from the sum of the advection and tilting terms is also shown. As in Figure 8.29, the illustration shows the horizontal cross-section of an updraft (pink) at midlevels and the relationship among ζ' (its sense is given by the curved blue arrows), S , $\bar{\omega}_h$, $\bar{v} - c$, and $\nabla_h \zeta'$. The lateral shifting of the ζ' field within the updraft cross-section depends on the orientation of $\bar{v} - c$ with respect to $\bar{\omega}_h$ (and $\nabla_h \zeta'$, which points in the opposite direction to $\bar{\omega}_h$). This orientation is related to whether the environmental horizontal vorticity is streamwise or crosswise.

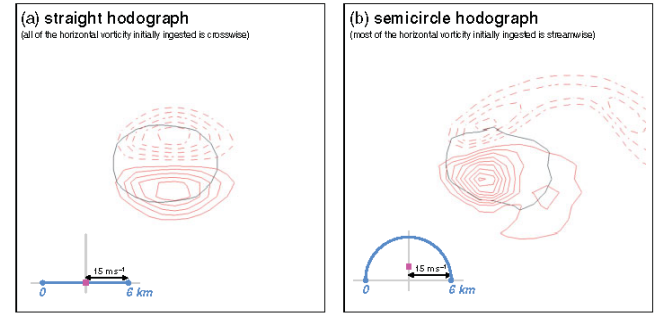
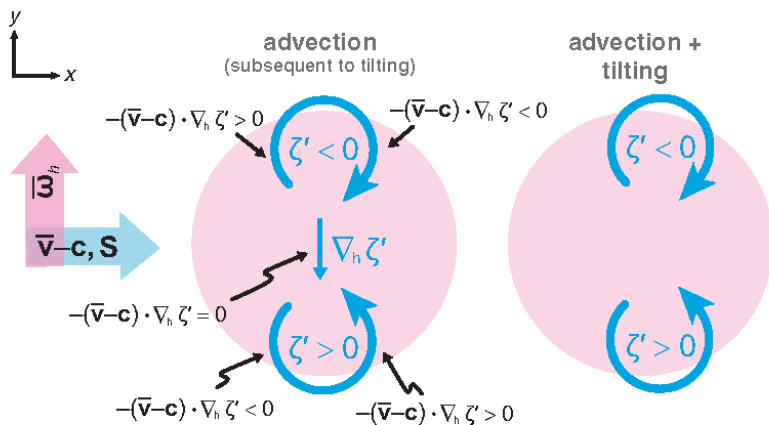


Figure 8.31 Vertical vorticity fields at $z = 5$ km at $t = 25$ min in numerical simulations in which an isolated storm is initiated using a warm bubble in an environment having (a) a straight hodograph and (b) a semicircular hodograph. Vertical vorticity contours are drawn every $2.5 \times 10^{-5} \text{ s}^{-1}$. Solid (dashed) contours indicate positive (negative) values, and the zero contour is suppressed. The thin black contour encloses the region where the vertical velocity exceeds 5 m s^{-1} . The sounding had approximately 2500 J kg^{-1} of CAPE. The hodographs are shown in each of the two panels; the magenta square indicates the mean updraft motion in the first 25 min of the simulations. In the straight-hodograph environment, the horizontal vorticity ingested in the early stages of storm development is purely crosswise. Note that the updraft is straddled by a couplet of cyclonic and anticyclonic vorticity of equal magnitude. In the semicircular hodograph environment, the updraft acquires net cyclonic rotation and the anticyclonic vorticity is predominantly within a downdraft.

(a) crosswise vorticity



Crosswise vorticity

$(\vec{v} - \vec{c})$ points in direction normal to \vec{w}_h

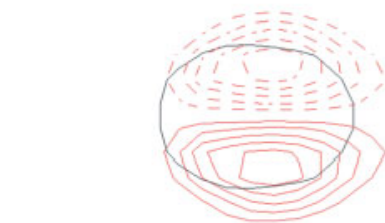
- Advection of vorticity = 0 at the location of maximum updraft

- No shifting of the vorticity couplet within the updraft in cross-shear direction.

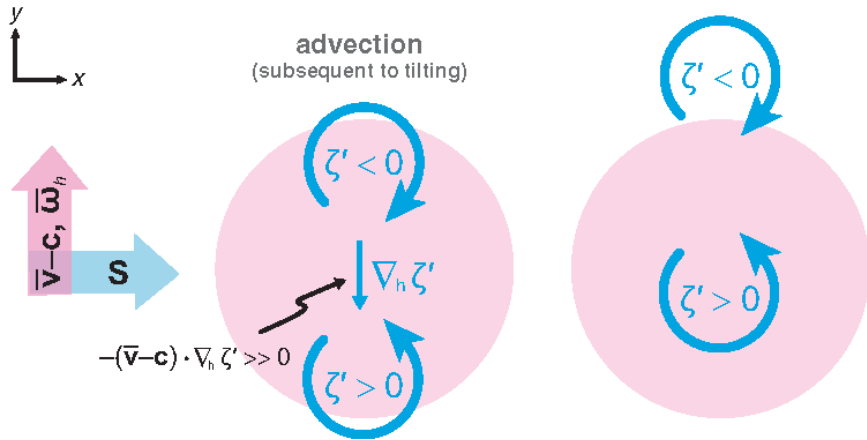
- Vorticity couplet is shifted just slightly down shear.

(a) straight hodograph

(all of the horizontal vorticity initially ingested is crosswise)

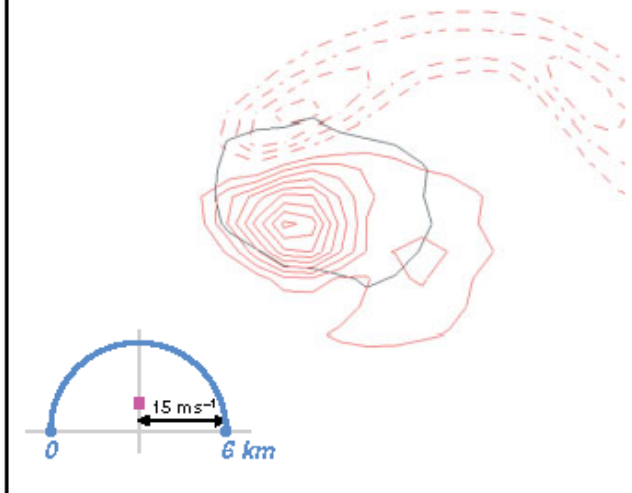


(b) streamwise vorticity



(b) semicircle hodograph

(most of the horizontal vorticity initially ingested is streamwise)



Stream wise vorticity

$(\vec{v}-\vec{c})$ points in direction parallel to $\vec{\omega}_h$.

- Advection of vorticity > 0 at the location of maximum updraft.

- Shifting of cyclonic vortex to location of maximum updraft.

- Anticyclonic vortex shifted outside of updraft, into downdraft.

- Co-locating of vortex and updraft permits (non-linear) vortex stretching.

Note: Also possible to favor the anticyclonic vortex, depending on orientation of $\vec{v}-\vec{c}$

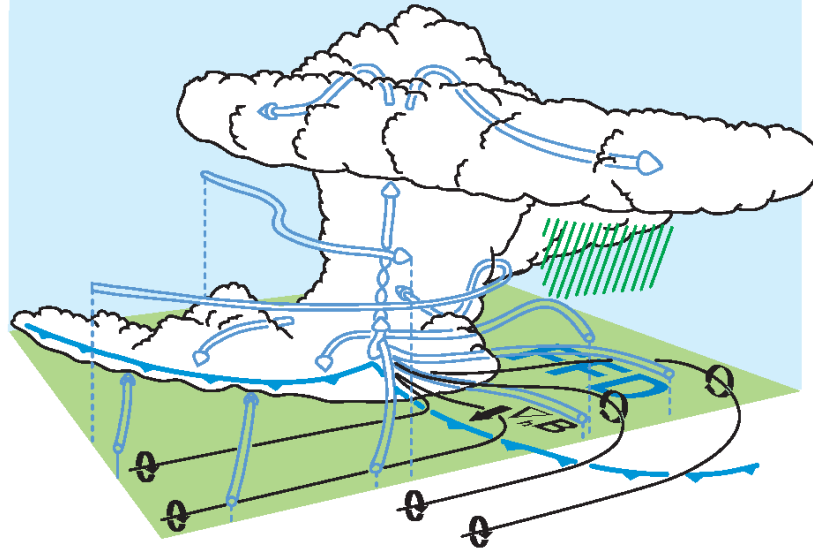


Figure 8.34 Schematic of a supercell thunderstorm in westerly mean shear, viewed from the southeast, at a stage when low-level rotation is intensifying. The cylindrical arrows depict the storm-relative winds. The black lines are vortex lines, with the sense of rotation indicated by the circular arrows. The blue barbed line marks the gust front. The orientation of the horizontal buoyancy gradient, $\nabla_h B$, is also indicated. (Adapted from Klemp [1987].)

Baroclinically generated horizontal vorticity

Once a storm gets going, can have internally generated horizontal vorticity from FFD outflows.

Can increase the available horizontal vorticity for tilting, especially at low levels

Results in a stronger, narrower updraft.

⇒ For tornado genesis in a mesocyclone, need some way to generate vertical vorticity at surface. It happens typically this way:

- 1) ~~FFD~~ Increased baroclinically generated horizontal vorticity from FFD.
- 2) Strong outflow boundary from RFD provides the source of vertical velocity to tilt horizontal velocity into vertical

So a rotating mesocyclone (supercell) is a necessary but not sufficient condition for a tornado.

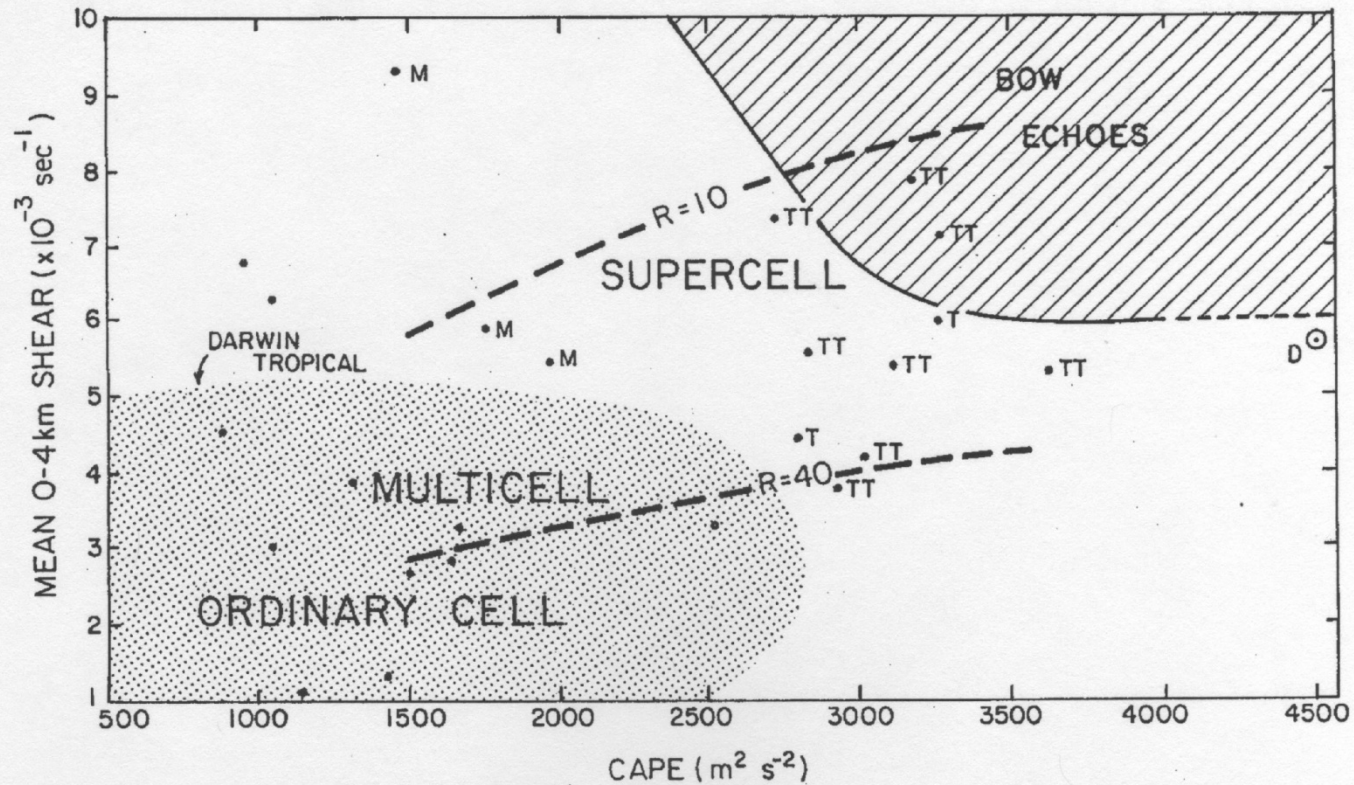
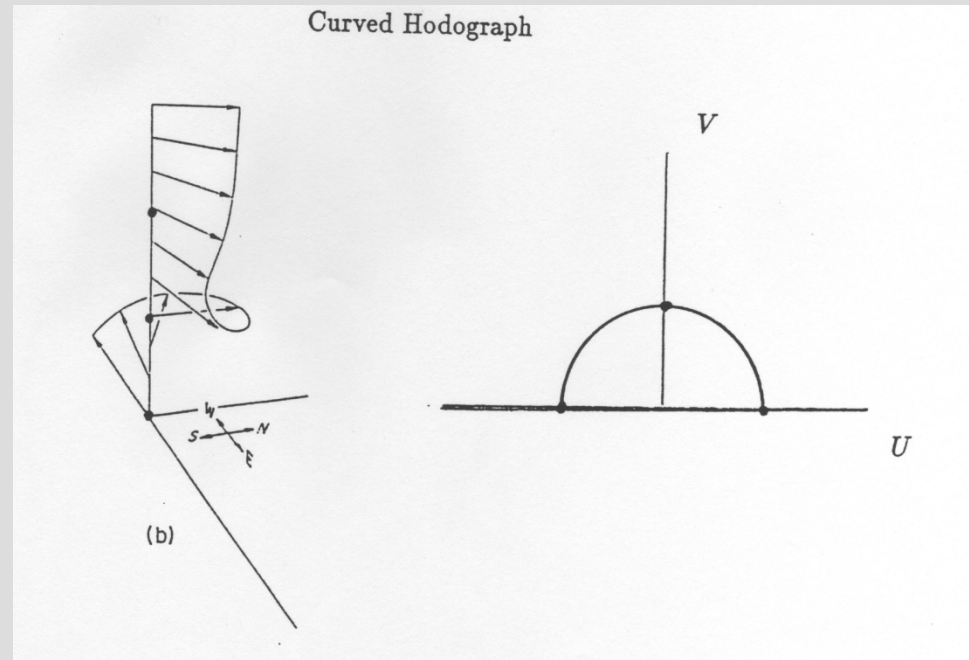
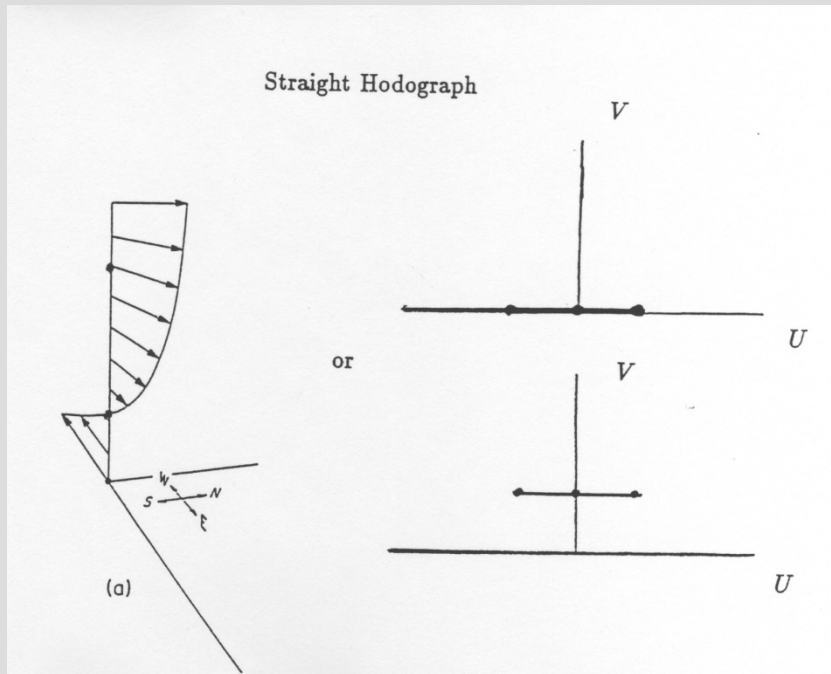


Figure 7.1: Types of convective elements as a function of mean vertical wind shear in the lowest 4 km and CAPE (from Rasmussen and Wilhelmson 1983). *M* represents a storm with a mesocyclone but no tornado, *T* a storm with one tornado, *TT* a storm with more than one tornado and an unmarked dot a storm without a mesocyclone. *D* represents mean conditions for derechos using data from Johns and Hirt (1987) and Johns et al. (1990). The heavy dashed lines indicate values of bulk Richardson number 10 and 40 (from Weisman and Klemp 1982, 1984, 1986). The shaded region indicates the approximate range of conditions found near Darwin, Australia, during the active and break monsoon periods (from Keenan and Carbone 1992). The hatched region indicates the range of conditions for bow echoes from Weisman 1993.

Unidirectional Shear vs. Directional Shear on Hodograph



In particular, observations show that a pronounced turning of the low-level shear vector is commonly found in proximity to supercell storms, especially those that produce tornadoes (e.g., Maddox 1976). This unique feature of midlatitude soundings can be expressed in terms of the *helicity* (H) of the environmental flow, where

$$H \equiv \boldsymbol{\omega} \cdot \mathbf{v},$$

3-D vort.
3-D velocity

and $\boldsymbol{\omega} = \nabla \times \mathbf{v}$. The importance of H for supercells or convection with strong rotation can be seen by considering the momentum equations in the form (following Lilly 1986)

$$\frac{\partial \mathbf{v}}{\partial t} + \mathbf{v} \cdot \nabla \mathbf{v} + \nabla \pi - b\mathbf{k} = 0, \quad (7.5)$$

Only vertical comp.

where $\pi \equiv (p - \bar{p})/\bar{\rho}$, $b = g(\theta_v - \bar{\theta}_v)/\bar{\theta}_v$ and overbar denotes a mean value. The advection term can be rewritten using the following identity:

$$\mathbf{v} \cdot \nabla \mathbf{v} = \nabla \frac{V^2}{2} + (\nabla \times \mathbf{v}) \times \mathbf{v}.$$

For purely helical flows $\boldsymbol{\omega}$ and \mathbf{v} are parallel. Then,

$$\mathbf{v} \cdot \nabla \mathbf{v} = \nabla \frac{V^2}{2}$$

and taking the curl of (7.5) yields

$$\frac{\partial \boldsymbol{\omega}}{\partial t} = \nabla b \times \mathbf{k}. \quad (7.6)$$

Since the RHS of (7.6) has no vertical component, vertically aligned helical flows can be long-lived and steady. In application, it is the storm-relative helicity of the environmental flow that is important (Davies-Jones 1984):

$$H = (\mathbf{v} - \mathbf{c}) \cdot \nabla \times \mathbf{v}, \quad (7.7)$$

where \mathbf{c} is the storm motion vector. Since the synoptic-scale flow is nearly horizontal, $(\mathbf{v} - \mathbf{c}) \cdot \nabla \times \mathbf{v} \approx \mathbf{k} \cdot (\mathbf{v} - \mathbf{c}) \times d\mathbf{v}/dz$, and therefore H is proportional to the area on a hodograph (Davies-Jones 1984).

In particular,

Vertical wind shear!

$$H(\mathbf{c}) = - \int_0^h \mathbf{k} \cdot (\mathbf{v} - \mathbf{c}) \times \frac{d\mathbf{v}}{dz} dz . \quad (7.8)$$

The integral in (7.8) is equivalent to twice the signed area swept out by the storm-relative wind vector between 0 and h (usually 3 km) on a hodograph (Fig. 7.3).

To estimate the storm motion vector (\mathbf{c}) in operational practice (e.g. from a morning sounding), consider pressure-weighted mean wind in lowest 5-6 km. In strong clockwise turning hodograph, add 5-10 m s⁻¹ to the right of the mean wind.

	<u>H (m² s⁻²)</u>
weak tornadoes	150-299
strong tornadoes	300-449
violent tornadoes	$\gtrsim 450$

$$H(\mathbf{c}) = - \int_0^h \mathbf{k} \cdot (\mathbf{v} - \mathbf{c}) \times \frac{d\mathbf{v}}{dz} dz . \quad (7.8)$$

The integral in (7.8) is equivalent to twice the signed area swept out by the storm-relative wind vector between 0 and h (usually 3 km) on a hodograph (Fig. 7.3).

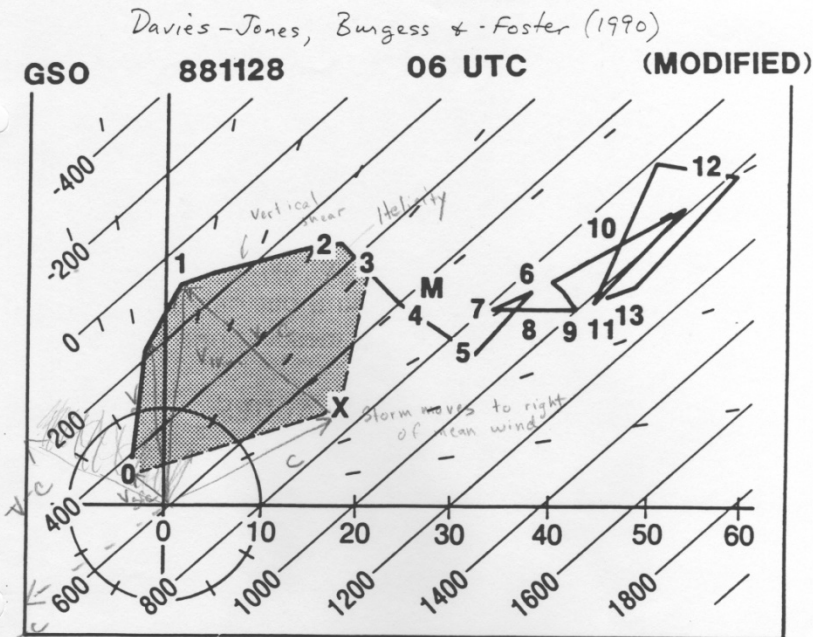



Fig. 7.3 Hodograph for Raleigh, NC tornado environment (Nov 28, 1988). The 00 UTC sounding at Greensboro has been modified slightly by backing the winds 10° in the lowest 1.5 km to reflect conditions believed to exist in the tornado environment. Speed circles are every $10\ m\ s^{-1}$ with dashed lines every 10° . Numbers along hodograph curve denote height AGL in km. Large X and M mark observed storm motion and mean wind between surface and 200 mb. The s-r helicity in the lowest 3 km is minus twice the shaded area (which is negative because the s-r wind turns clockwise with height). Straight lines parallel to 0-3 km shear vector are contours of helicity for this hodograph as a function of storm motion, i.e., the location of X. For observed storm motion of 240° at $20\ m\ s^{-1}$, the helicity was $719\ m^2s^{-2}$ for the modified and $615\ m^2s^{-2}$ for the unmodified hodograph.

Mesoscale dynamics of supercell thunderstorms

Has mainly to do with dynamic pressure effects and tilting of horizontal vorticity in an environment of high (rotational) vertical shear, assuming you have the requisite thermodynamic conditions present.

Simplified equations of motion for convection on mesoscale

	<u>Full equation</u>		<u>Linearize, Boussinesq approx.</u>
U momentum	$\frac{Du}{Dt} = -\frac{1}{\rho} \frac{\partial p}{\partial x}$		$\frac{Du}{Dt} = -\frac{1}{\rho} \frac{\partial p'}{\partial x}$
V momentum	$\frac{Dv}{Dt} = -\frac{1}{\rho} \frac{\partial p}{\partial y}$		$\frac{Dv}{Dt} = -\frac{1}{\rho} \frac{\partial p'}{\partial y}$
W momentum	$\frac{Dw}{Dt} = -\frac{1}{\rho} \frac{\partial p}{\partial z} - g$		$\frac{Dw}{Dt} = -\frac{1}{\rho} \frac{\partial p'}{\partial z} + B$

IMPORTANT ASIDE: Absolutely no Coriolis effects here! So any rotations in supercell storms due ONLY to mesoscale dynamics—NOT the synoptic scale!

$$B = -\frac{\rho'}{\rho} g \quad \text{Buoyancy}$$

Differentiate u and v momentum equations with respect to x and y, respectively, then add together..

Add w momentum equation, differentiated with respect to z and assuming constant mean density, to get a **divergence equation**:

$$\frac{D}{Dt}(\nabla \bullet \bar{\mathbf{v}}) + \frac{1}{\rho} \nabla^2 p' = \left[\left(\frac{\partial u}{\partial x} \right)^2 + \left(\frac{\partial v}{\partial y} \right)^2 + \left(\frac{\partial w}{\partial z} \right)^2 + 2 \frac{\partial u}{\partial y} \frac{\partial v}{\partial x} + 2 \frac{\partial u}{\partial z} \frac{\partial w}{\partial x} + 2 \frac{\partial v}{\partial z} \frac{\partial w}{\partial y} \right] + \frac{\partial B}{\partial z}$$

Invoking a shallow water assumption, our first term on LHS vanishes because:

$$\nabla \bullet \bar{\mathbf{v}} = \frac{\partial u}{\partial x} + \frac{\partial v}{\partial y} + \frac{\partial w}{\partial z} = 0$$

Linearize about the following state:

$$u = \bar{u}(z) + u'(x, y, z, t)$$

$$v = \bar{v}(z) + v'(x, y, z, t)$$

$$w = w'(x, y, z, t)$$

Assume a linearly varying mean vertical wind profile of u and v, for simplicity.

Laplacian equation for pressure perturbation = **dynamic pressure + buoyancy**

$$\frac{1}{\rho} \nabla^2 p' = - \left[\left(\frac{\partial u'}{\partial x} \right)^2 + \left(\frac{\partial v'}{\partial y} \right)^2 + \left(\frac{\partial w'}{\partial z} \right)^2 + 2 \left(\frac{\partial u'}{\partial y} \frac{\partial v'}{\partial x} + \frac{\partial u'}{\partial z} \frac{\partial w'}{\partial x} + \frac{\partial v'}{\partial z} \frac{\partial w'}{\partial y} + \frac{\partial \bar{u}}{\partial z} \frac{\partial w'}{\partial x} + \frac{\partial \bar{v}}{\partial z} \frac{\partial w'}{\partial y} \right) \right] + \frac{\partial B}{\partial z}$$

$$p' = p'_{dyn} + p'_B = p'_{dynL} + p'_{dynNL} + p'_B$$

Linear dynamic contribution: Interaction of environmental shear with updraft vertical velocity (i.e. rotation of horizontal environmental vorticity into vertical)

$$\nabla^2 p'_{dynL} \propto - \left[\frac{\partial \bar{u}}{\partial z} \frac{\partial w'}{\partial x} + \frac{\partial \bar{v}}{\partial z} \frac{\partial w'}{\partial y} \right] = - \frac{\partial \bar{\mathbf{v}}_H}{\partial z} \cdot \nabla_H w'$$

Non-linear dynamic contributions: Fluid extension terms and shear terms

$$\nabla^2 p'_{dynNL} \propto - \left[\left(\frac{\partial u'}{\partial x} \right)^2 + \left(\frac{\partial v'}{\partial y} \right)^2 + \left(\frac{\partial w'}{\partial z} \right)^2 + 2 \left(\frac{\partial u'}{\partial y} \frac{\partial v'}{\partial x} + \frac{\partial u'}{\partial z} \frac{\partial w'}{\partial x} + \frac{\partial v'}{\partial z} \frac{\partial w'}{\partial y} \right) \right]$$

Fluid extension

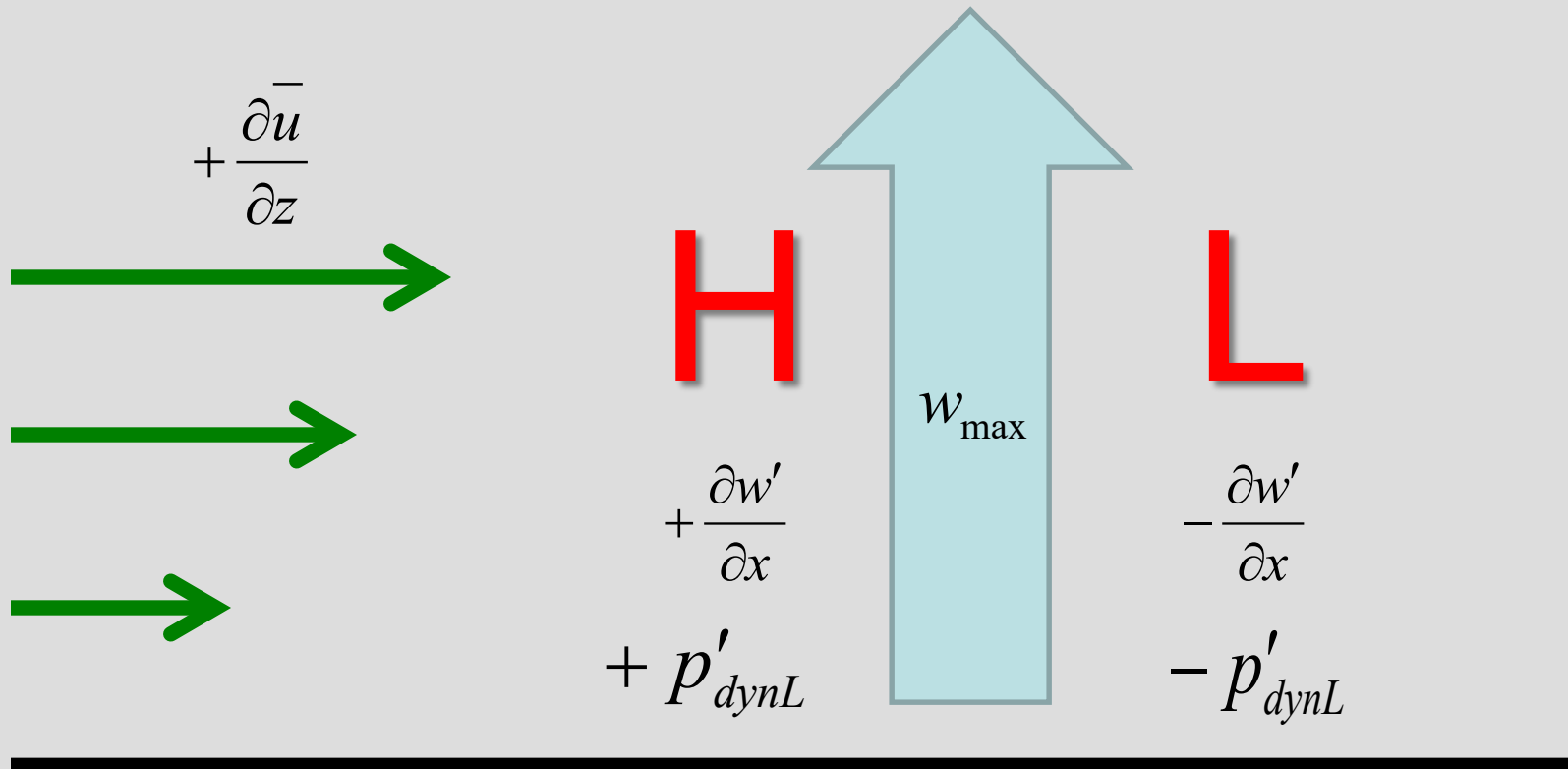
Shear

Contributions to dynamic pressure by linear dynamics

Since a Laplacian tends to change the sign of the variable on which it operates:

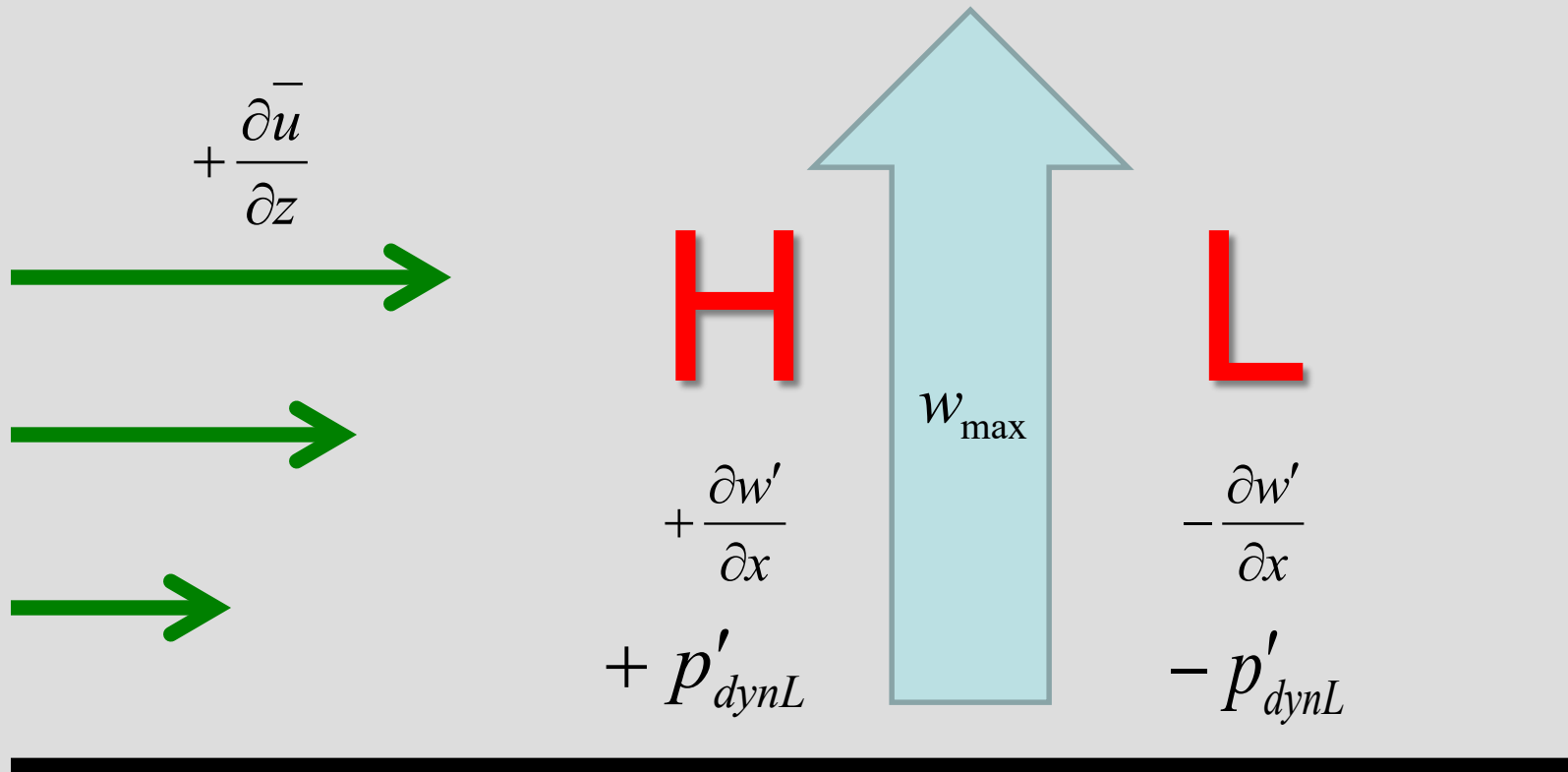
$$p'_{dynL} \propto \frac{\partial \bar{v}_H}{\partial z} \cdot \nabla_H w'$$

For an updraft in an environment of positive unidirectional zonal shear,
 Positive perturbation pressure on upshear side of updraft
 Negative perturbation pressure on downshear side of updraft

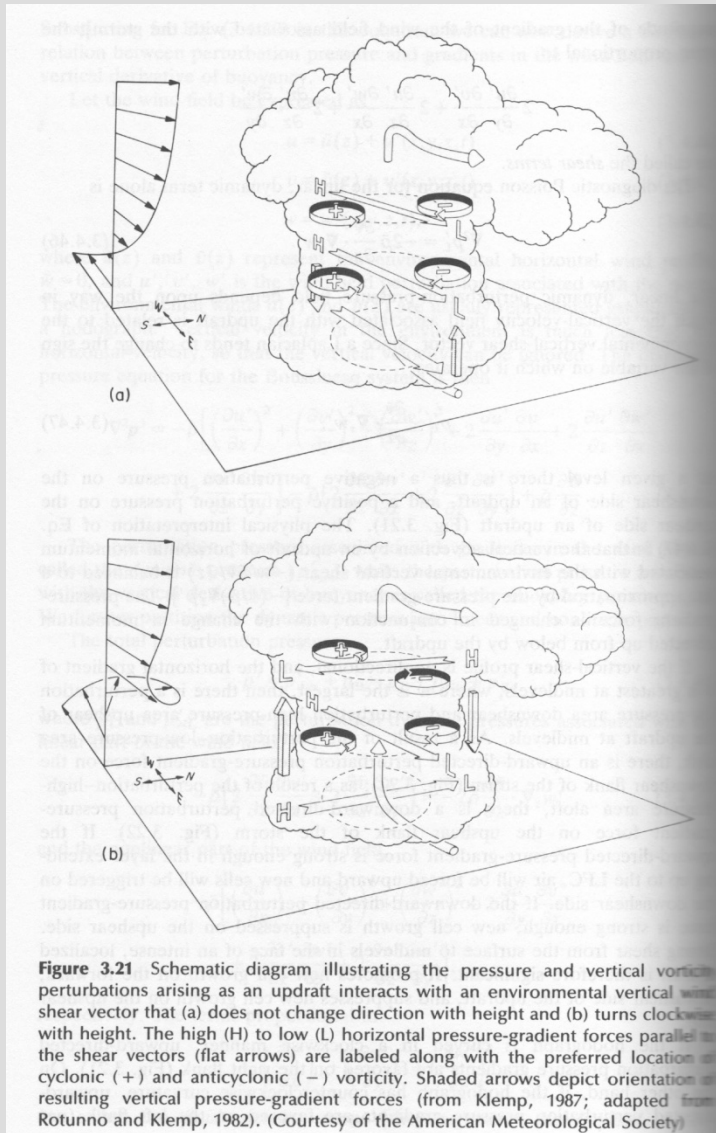


$$p'_{dynL} \propto \frac{\partial \bar{v}_H}{\partial z} \cdot \nabla_H w'$$

Physical interpretation: Vertical advection by an updraft of horizontal momentum associated with environmental shear is balanced by pressure gradient force.



Effects of linear pressure perturbation terms



Unidirectional shear

For a maximum updraft velocity in mid-levels, perturbation high pressure upshear, low pressure downshear. **Helps promote new cell growth downwind of the updraft in front of the storm.**

Directional (clockwise) shear

Upward directed pressure gradients are favored on more on the right flank of the storm. Opposite for counterclockwise shear.

Almost always a clockwise rotating shear profile for supercell thunderstorms in United States.

(Bluestein)

Contribution to pressure perturbation by non-linear dynamics

Shearing terms:

$$\nabla^2 p'_{dynNLshear} \propto -2 \left(\frac{\partial u'}{\partial y} \frac{\partial v'}{\partial x} + \frac{\partial u'}{\partial z} \frac{\partial w'}{\partial x} + \frac{\partial v'}{\partial z} \frac{\partial w'}{\partial y} \right)$$

Can express with deformation and vorticity terms in all directions:

$$= -\frac{1}{2} \left[\left(\frac{\partial v'}{\partial x} + \frac{\partial u'}{\partial y} \right)^2 - \left(\frac{\partial v'}{\partial x} - \frac{\partial u'}{\partial y} \right)^2 + \left(\frac{\partial u'}{\partial z} + \frac{\partial w'}{\partial x} \right)^2 - \left(\frac{\partial u'}{\partial z} - \frac{\partial w'}{\partial x} \right)^2 + \left(\frac{\partial w'}{\partial y} + \frac{\partial v'}{\partial z} \right)^2 - \left(\frac{\partial w'}{\partial y} - \frac{\partial v'}{\partial z} \right)^2 \right]$$

Shearing terms:

$$\nabla^2 p'_{dynNLshear} \propto -2 \left(\frac{\partial u'}{\partial y} \frac{\partial v'}{\partial x} + \frac{\partial u'}{\partial z} \frac{\partial w'}{\partial x} + \frac{\partial v'}{\partial z} \frac{\partial w'}{\partial y} \right)$$

Can express with deformation and vorticity terms in all directions:

$$= -\frac{1}{2} \left[\left(\frac{\partial v'}{\partial x} + \frac{\partial u'}{\partial y} \right)^2 - \left(\frac{\partial v'}{\partial x} - \frac{\partial u'}{\partial y} \right)^2 + \left(\frac{\partial u'}{\partial z} + \frac{\partial w'}{\partial x} \right)^2 - \left(\frac{\partial u'}{\partial z} - \frac{\partial w'}{\partial x} \right)^2 + \left(\frac{\partial w'}{\partial y} + \frac{\partial v'}{\partial z} \right)^2 - \left(\frac{\partial w'}{\partial y} - \frac{\partial v'}{\partial z} \right)^2 \right]$$

Consider tilting of unidirectional shear by an updraft, such that all deformation terms and horizontal vorticity terms (i.e. crossed out terms) are zero. **All that is left is vertical vorticity.**

$$\nabla^2 p'_{dynNLshear} \propto \left(\frac{\partial v'}{\partial x} - \frac{\partial u'}{\partial y} \right)^2 = \zeta'^2$$

$$p'_{dynNLshear} \propto -\zeta'^2$$

Again, sign changes with Laplacian inversion

Result: Non-linear shearing terms produce low perturbation pressure in the vicinity of mid-level anticyclonic and cyclonic vorticity induced by the updraft.

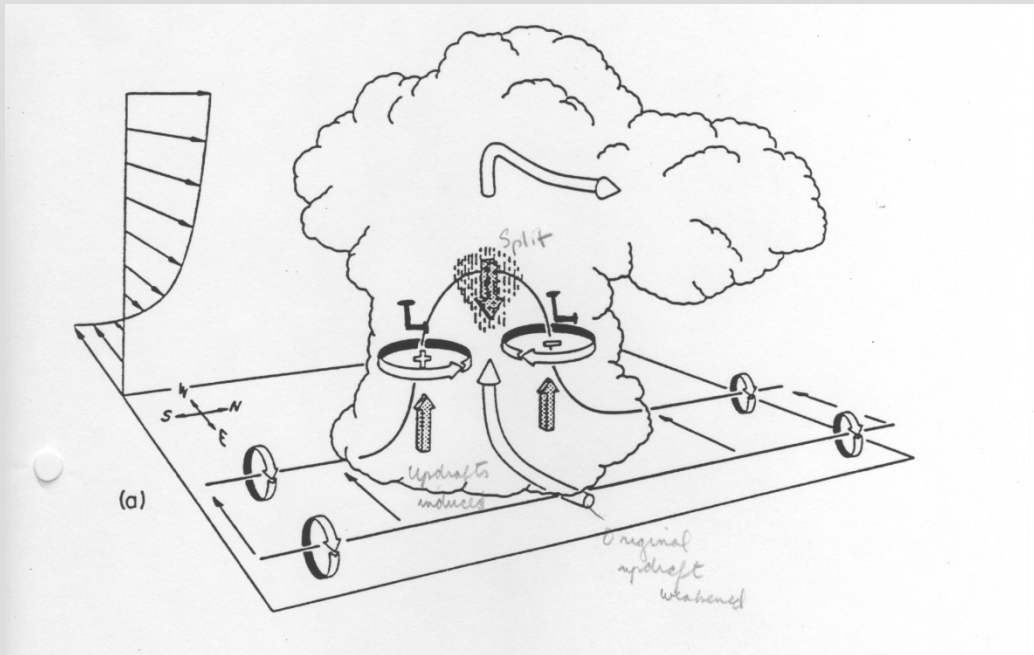
Effect of non-linear pressure perturbation terms (shearing)

In unidirectional shear

Have formation of mid-level vortices at storm flanks.
Results from tilting of horizontal vorticity of the environment by updrafts results in perturbation low pressure.

This DOES NOT depend on the direction of rotation!

The upward directed pressure gradient at storm flanks will tend to enhance updrafts at the sides of the storm.



Storm splitting process

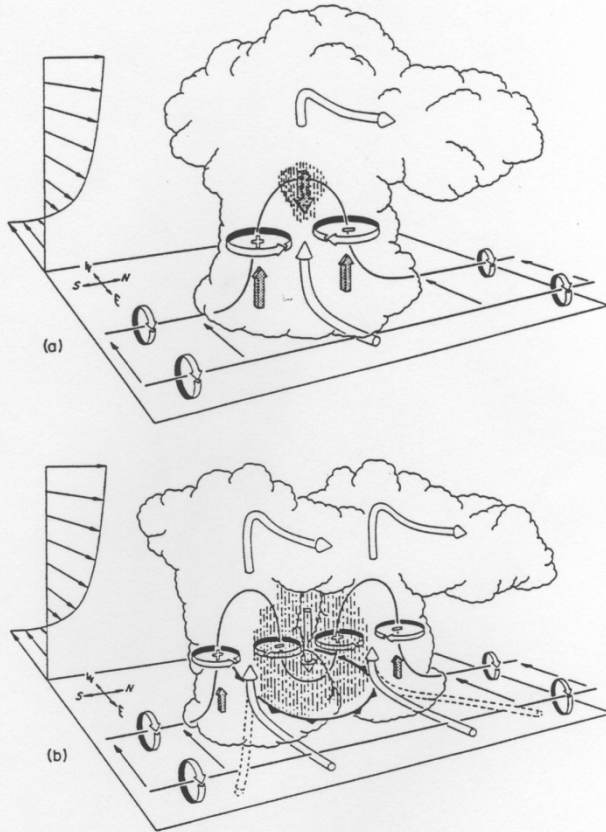


Figure 46. Schematic depicting how a typical vortex tube contained within (westerly) environmental shear is deformed as it interacts with a convective cell (viewed from the southeast). Cylindrical arrows show the direction of cloud- relative airflow, and heavy solid lines represent vortex lines with the sense of rotation indicated by circular arrows. Shaded arrows represent the forcing influences that promote new updraft and downdraft growth. Vertical dashed lines denote regions of precipitation. (a) Initial stage: Vortex tube loops into the vertical as it is swept into the updraft. (b) Splitting stage: Downdraft forming between the splitting updraft cell tilts vortex tubes downward, producing two vortex pairs. The barbed line at the surface marks the boundary of the cold air spreading out beneath the storm (from Klemp, 1987).

A downdraft in the center of the storm starts to weaken the updraft. Strongest vertical motion becomes more favored at right and left flanks.

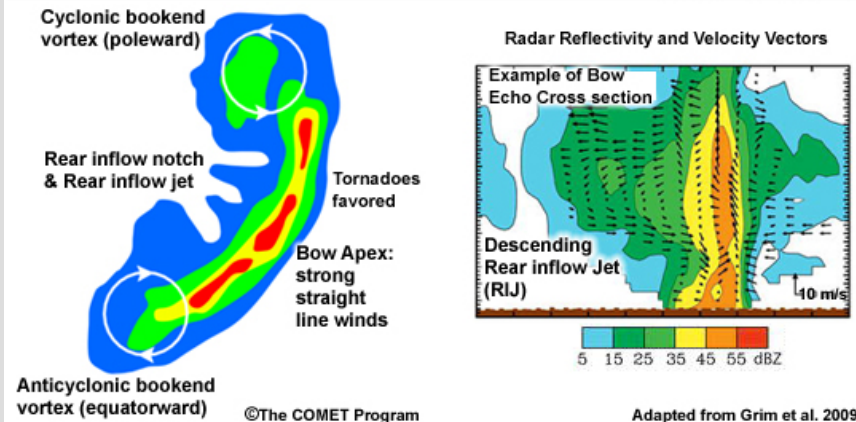
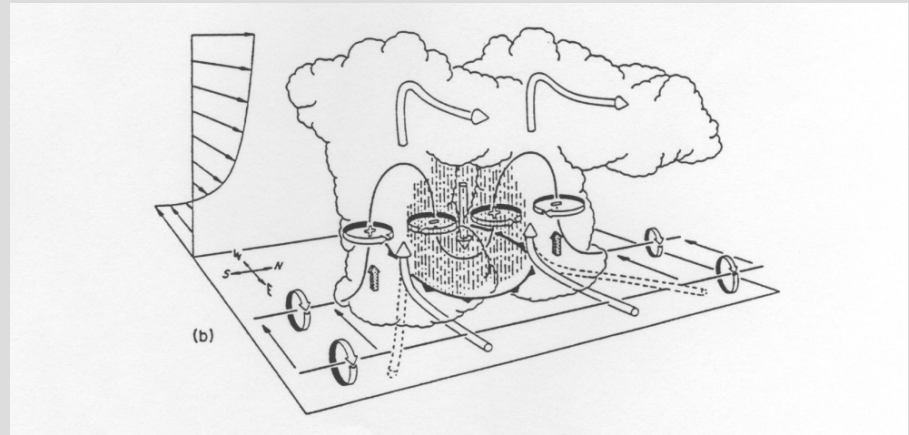
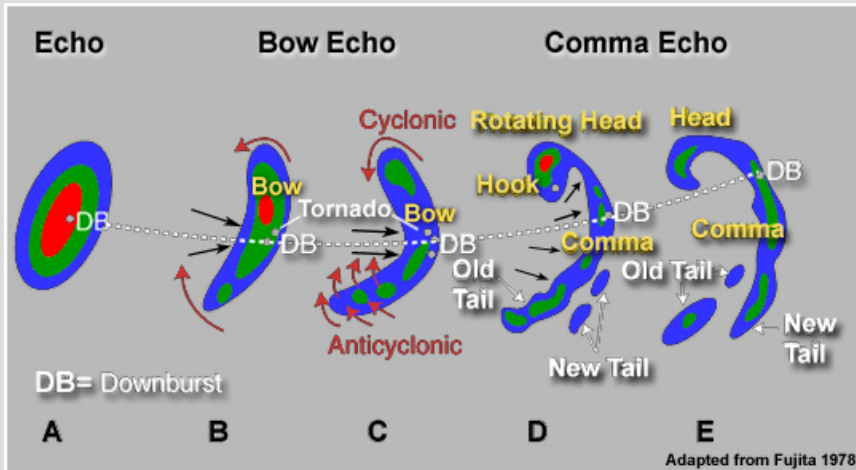
The downdraft splits the storm into two:

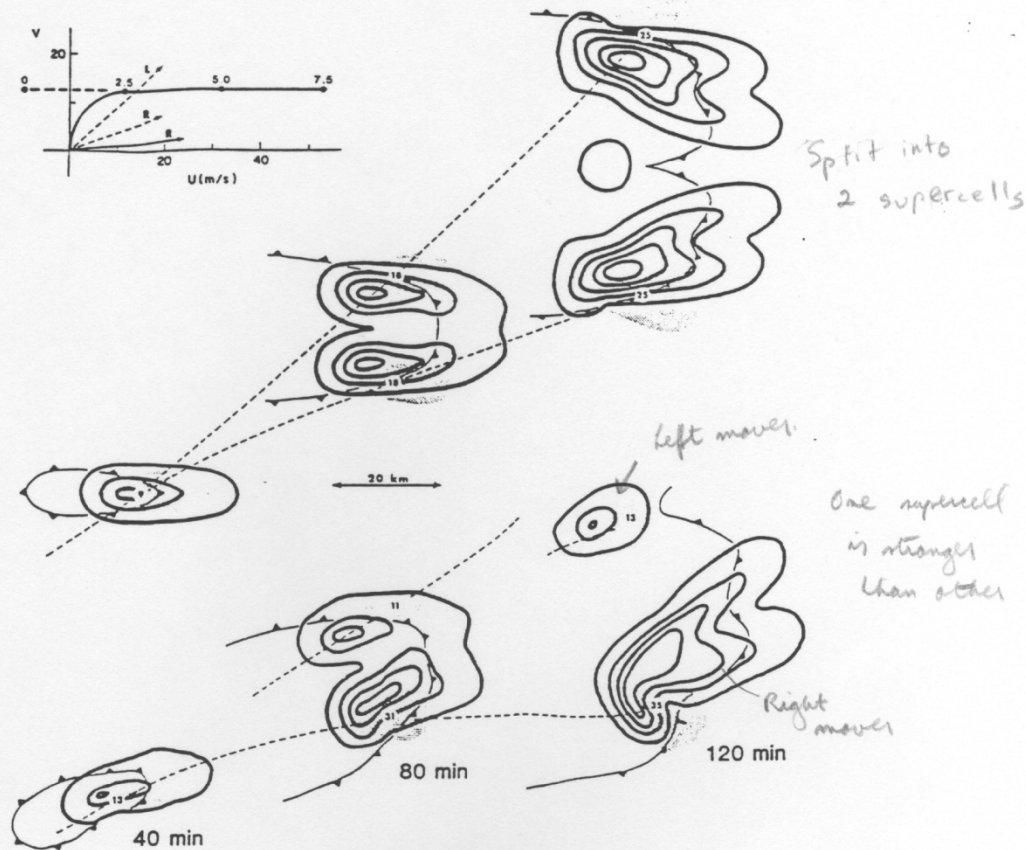
Right mover: cyclonically rotating on the right flank

Left mover: anticyclonically rotating on the left flank.

The aforementioned linear perturbation pressure effects will favor the development of the right mover in an environment with clockwise rotating shear.

High CAPE, unidirectional shear typically associated with bow echo, derecho events → quasi-linear





UNIDIRECTIONAL
SHEAR: Left and
right movers
equally favored

CLOCKWISE
ROTATING SHEAR
PROFILE: Favors
right mover

Figure 6 Plan views of numerically simulated thunderstorm structures at 40, 80, and 120 min for two environmental wind profiles (displayed at upper left) having wind shear between the surface and 7.5 km. The storm system in the lower portion of the figure evolves in response to the wind profile in which S turns clockwise with height between the ground and 2.5 km (heavy solid line in wind plot), while the upper system develops when S is unidirectional (same wind profile except following the heavy dashed line below 2.5 km). The plan views depict the low-level (1.8 km) rainwater field (similar to radar reflectivity) contoured at 2 g kg^{-1} intervals, the midlevel (4.6 km) updraft (shaded regions), and the location of the surface cold-air outflow boundary (barbed lines). The maximum updraft velocity is labeled (in m s^{-1}) within each updraft at each time. The dashed lines track the path of each updraft center. Arrows in the wind plot indicate the supercell propagation velocities for the unidirectional (dashed) and turning (solid) wind shear profiles. (Adapted from Klemp & Weisman 1983.)

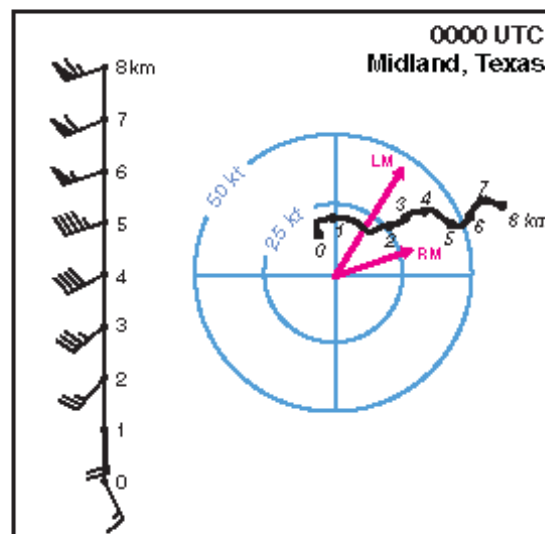
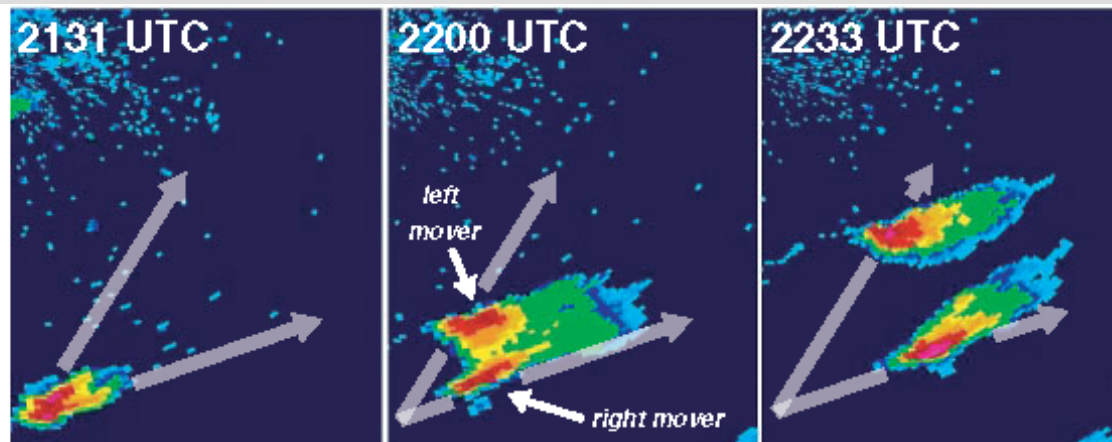


Figure 8.37 Sequence of radar reflectivity images from the Clovis, NM, WSR-88D on 19 April 2004, depicting a developing supercell storm splitting into right- and left-moving supercells. The vertical wind profile and hodograph from Midland, TX, at 0000 UTC 20 April are displayed as well. Numerals along the hodograph indicate altitudes above ground level in kilometers, and the storm motions are also indicated on the hodograph ('RM' and 'LM' are the motion vectors of the right- and left-moving supercells, respectively). The hodograph is fairly straight overall. It is therefore not surprising that the right- and left-moving supercells that developed from the splitting process were comparable in intensity.

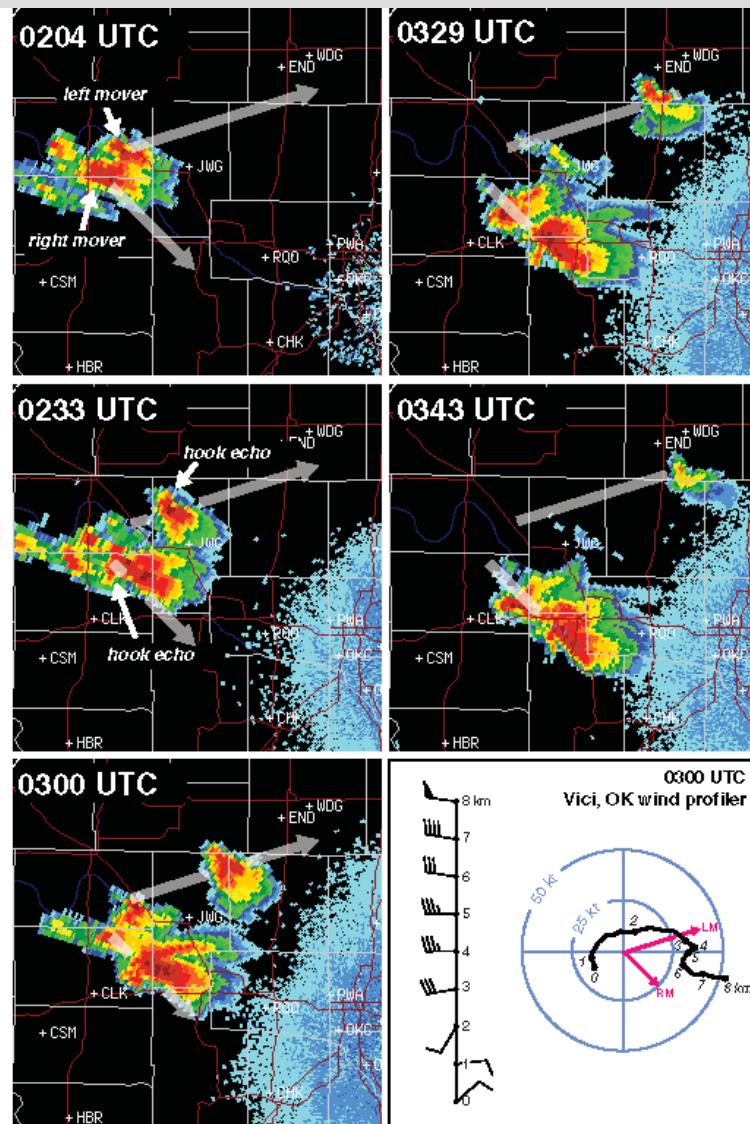
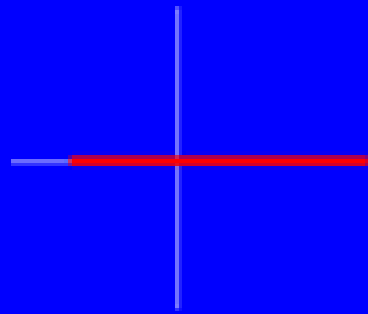


Figure 8.42 Left- and right-moving supercells following an episode of storm-splitting on 1 June 2008 in western Oklahoma. Note the intensification (weakening) of the right- (left-) mover following the splitting of the original cell. The broad gray arrows indicate the storm motions. The vertical wind profile and hodograph from the nearby Vici, OK, wind profiler are displayed in the bottom right panel. Numerals along the hodograph indicate altitudes above ground level in kilometers, and the storm motions are also indicated on the hodograph ("RM" and "LM" are the motion vectors of the right- and left-movers, respectively). The hodograph has substantial curvature, such that the shear vector veers with height in the lowest 4 km. It is therefore not surprising that the right-mover was dominant in this case.

Supercell Propagation Behaviour as a Function of Hodograph Shape



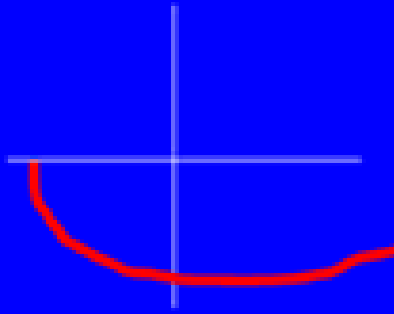
Left-mover



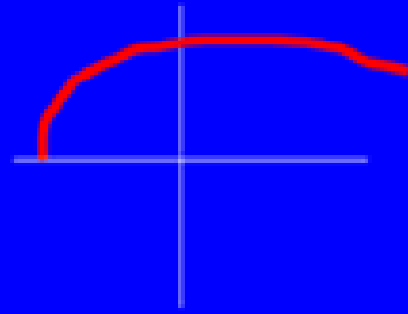
Split



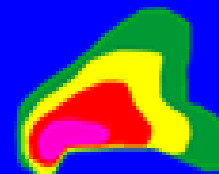
Right-mover



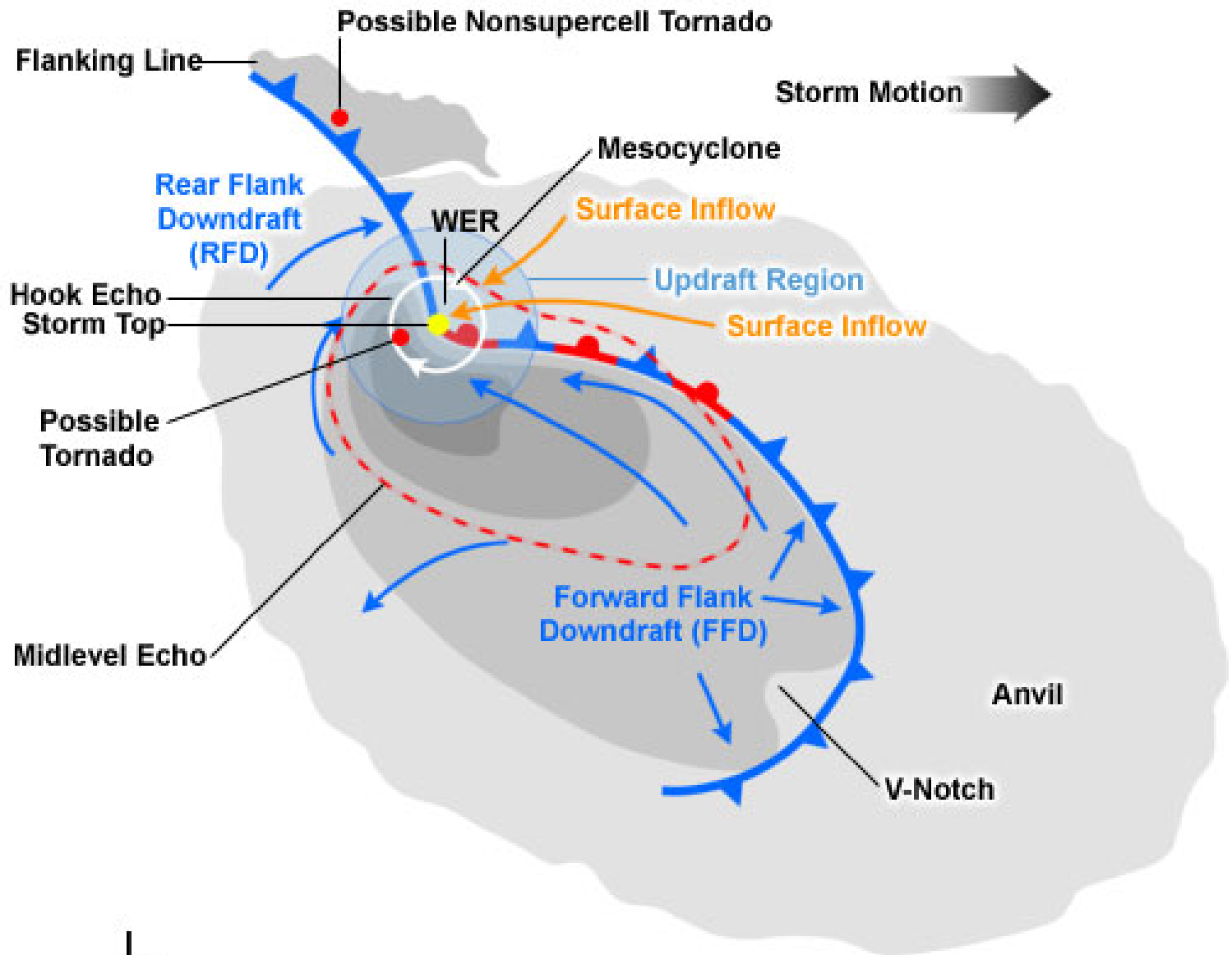
Left-mover



Right-mover



Left-Moving Supercell Schematic in the Southern Hemisphere

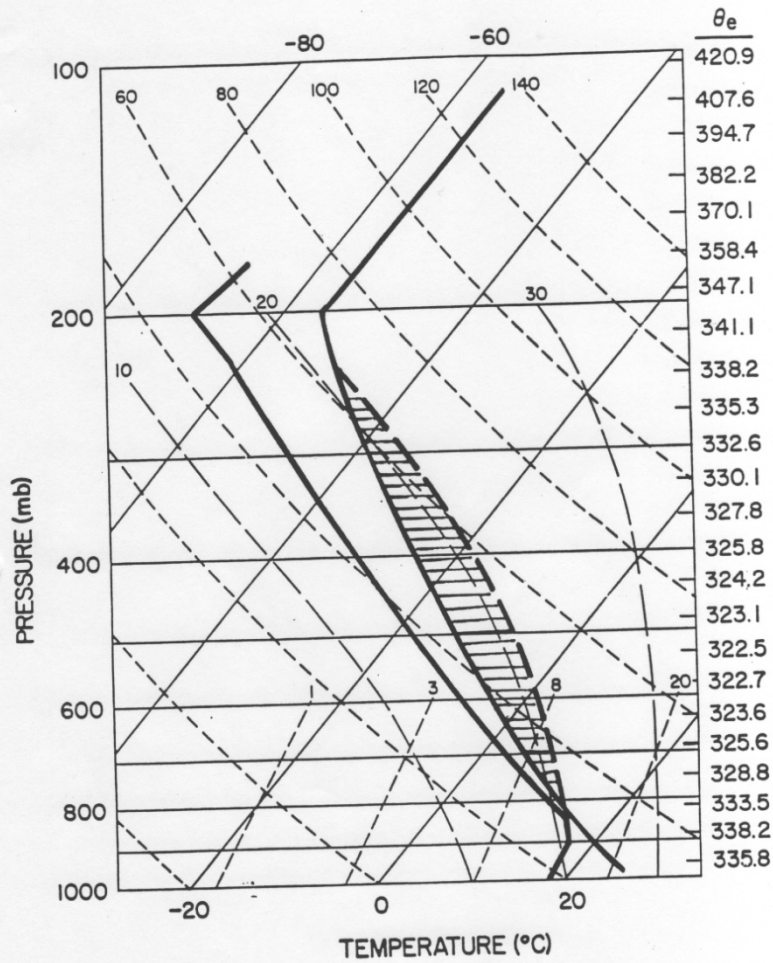


0 10 km

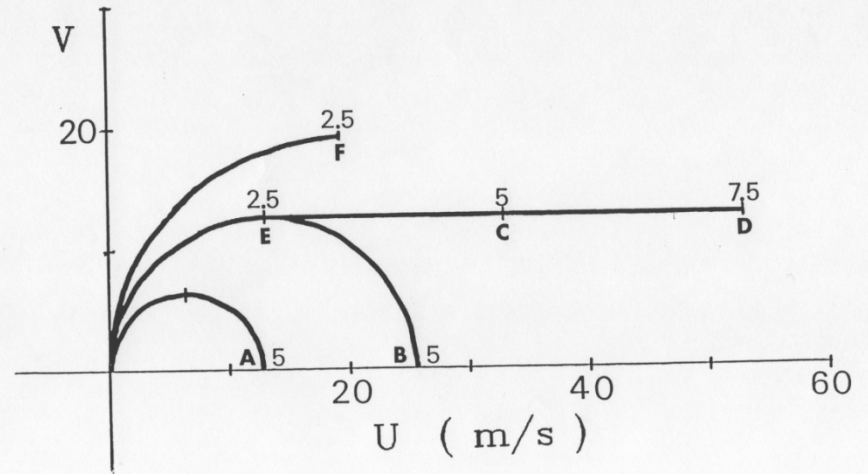
KLEMP-WILHELMSON
3-D NUMERICAL CLOUD MODEL

- * ***Compressible Equations of Motion***
- * ***Prognostic Variables: $u, v, w, t, p, q_v, q_c, q_r$***
- * ***Kessler-type parameterization for microphysics
(no ice)***
- * ***Subgrid scale turbulence parameterization
based on a turbulence energy equation***
- * ***Open lateral boundary conditions***
- * ***Storms initiated by a symmetric warm bubble
within a horizontally homogeneous environment,
characterized by specified vertical profiles of
wind, moisture, and temperature***

Constant idealized sounding



Vary wind shear profile (as seen in hodograph)



Bulk Richardson number (R)

Since storm strength is dependent on BOTH instability and shear, can define a bulk Richardson number (R).

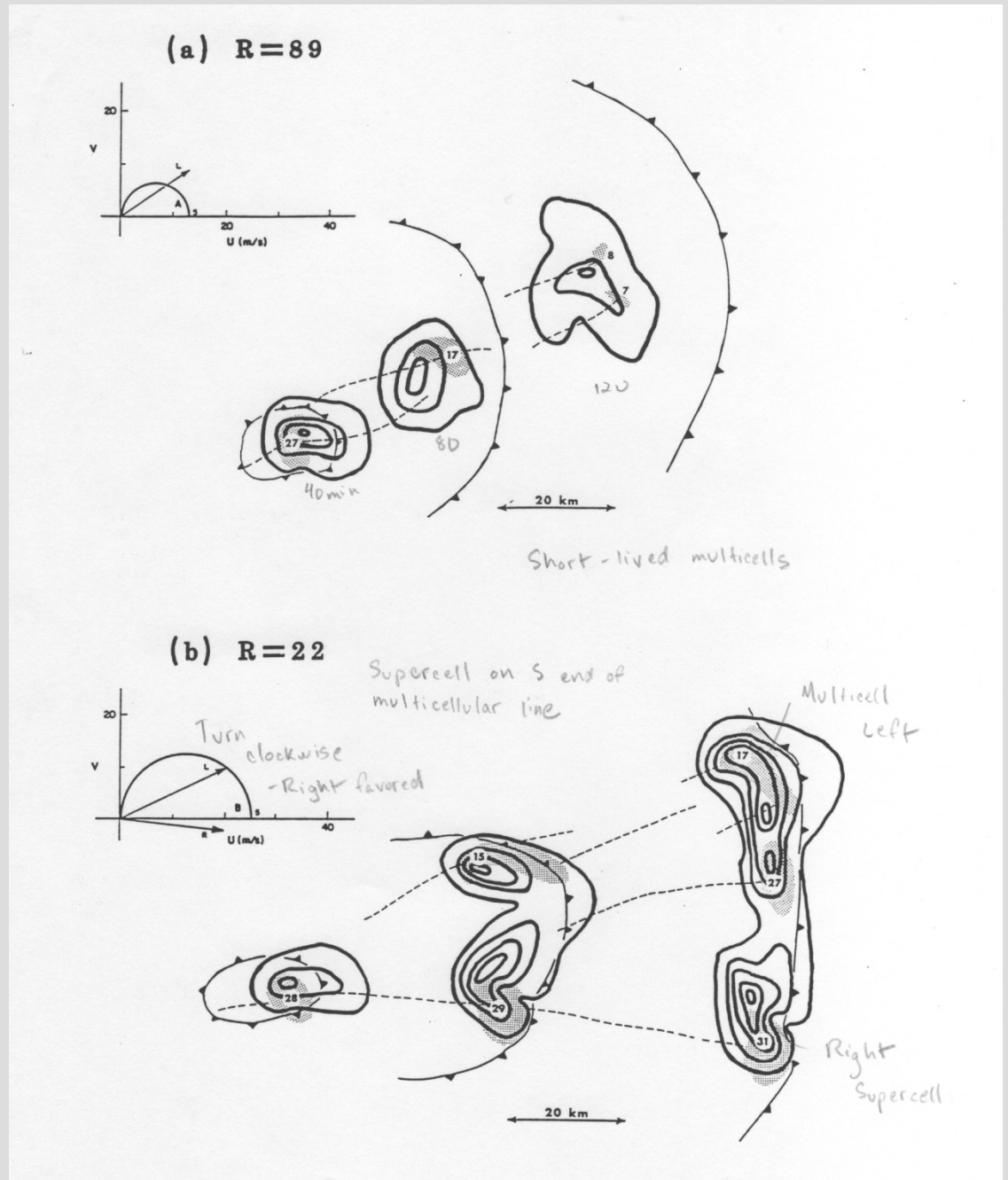
$$R = \text{CAPE}/S^2$$

$$S^2 = \frac{1}{2} (u_{6\text{km}} - u_{500\text{m}})^2$$

This measure gives some indication of the potential for organized convection.

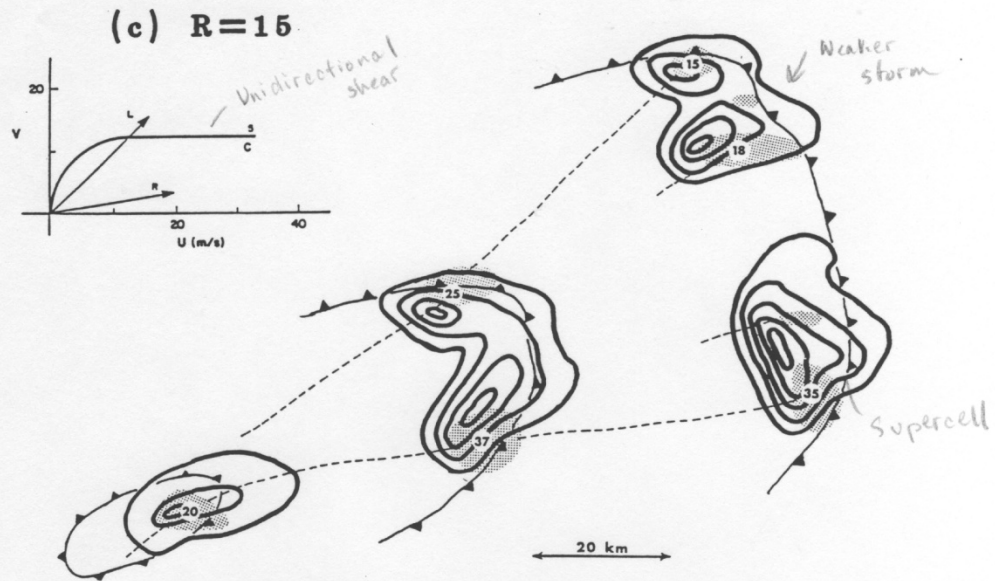
Supercell (tornadic) thunderstorms tend to form with $10 < R < 40$. So need some sort of optimal balance of CAPE vs. shear to get most intense kinds of thunderstorms.

CASE A

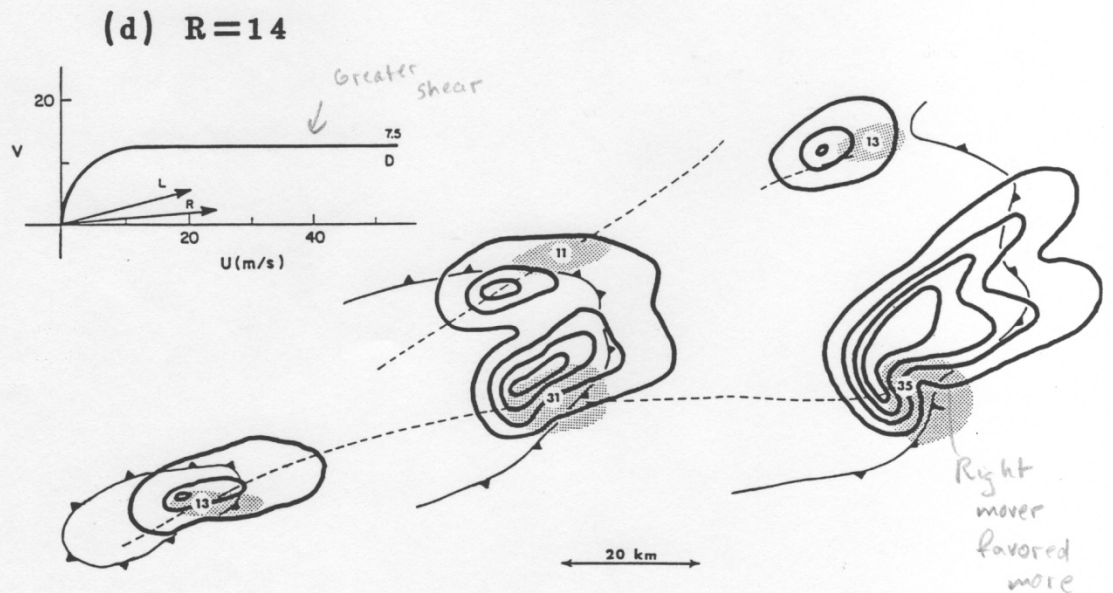


CASE B

CASE C

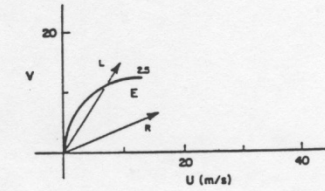


CASE D

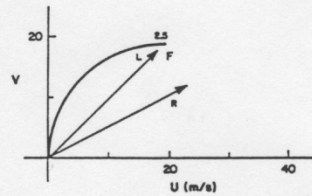
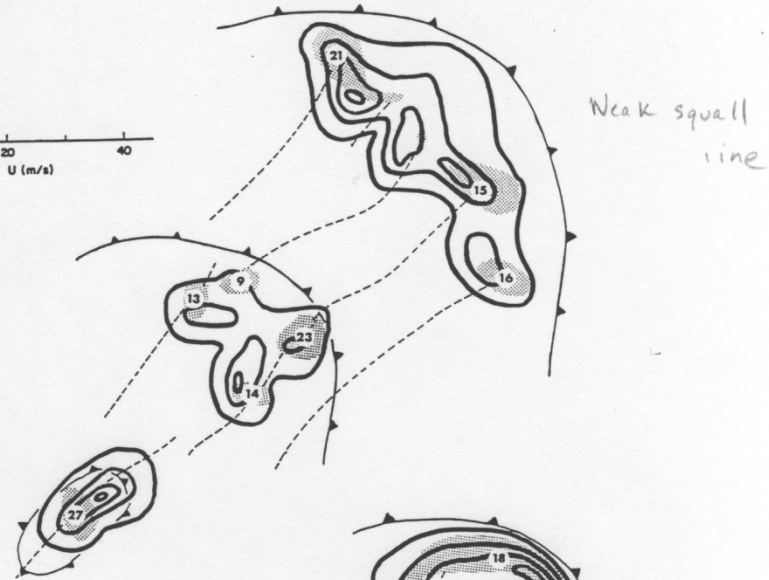


CASE E

(e) $R=34$

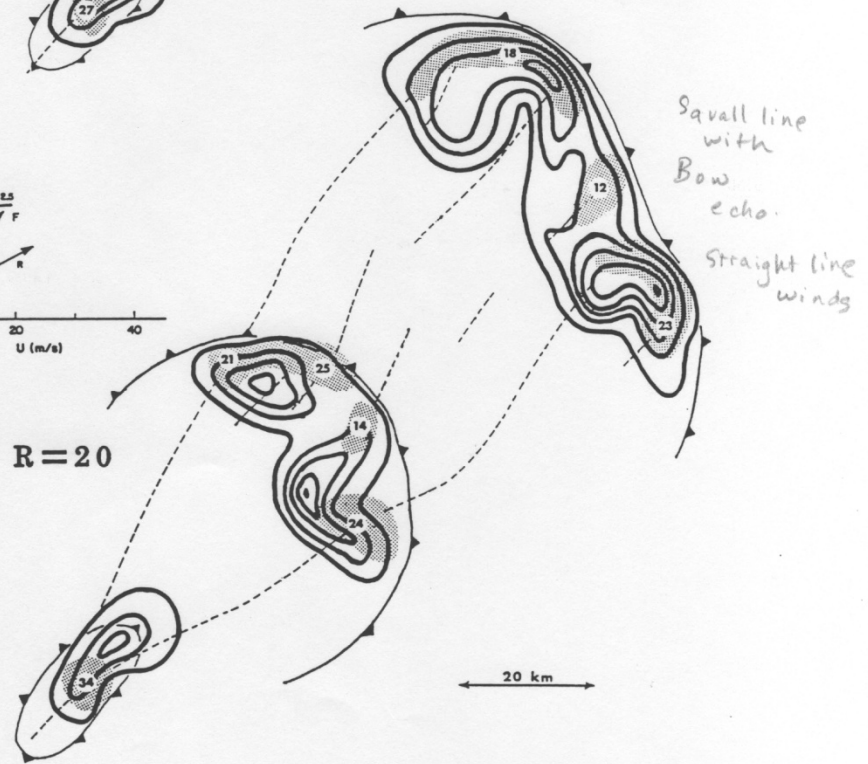


Shear truncated



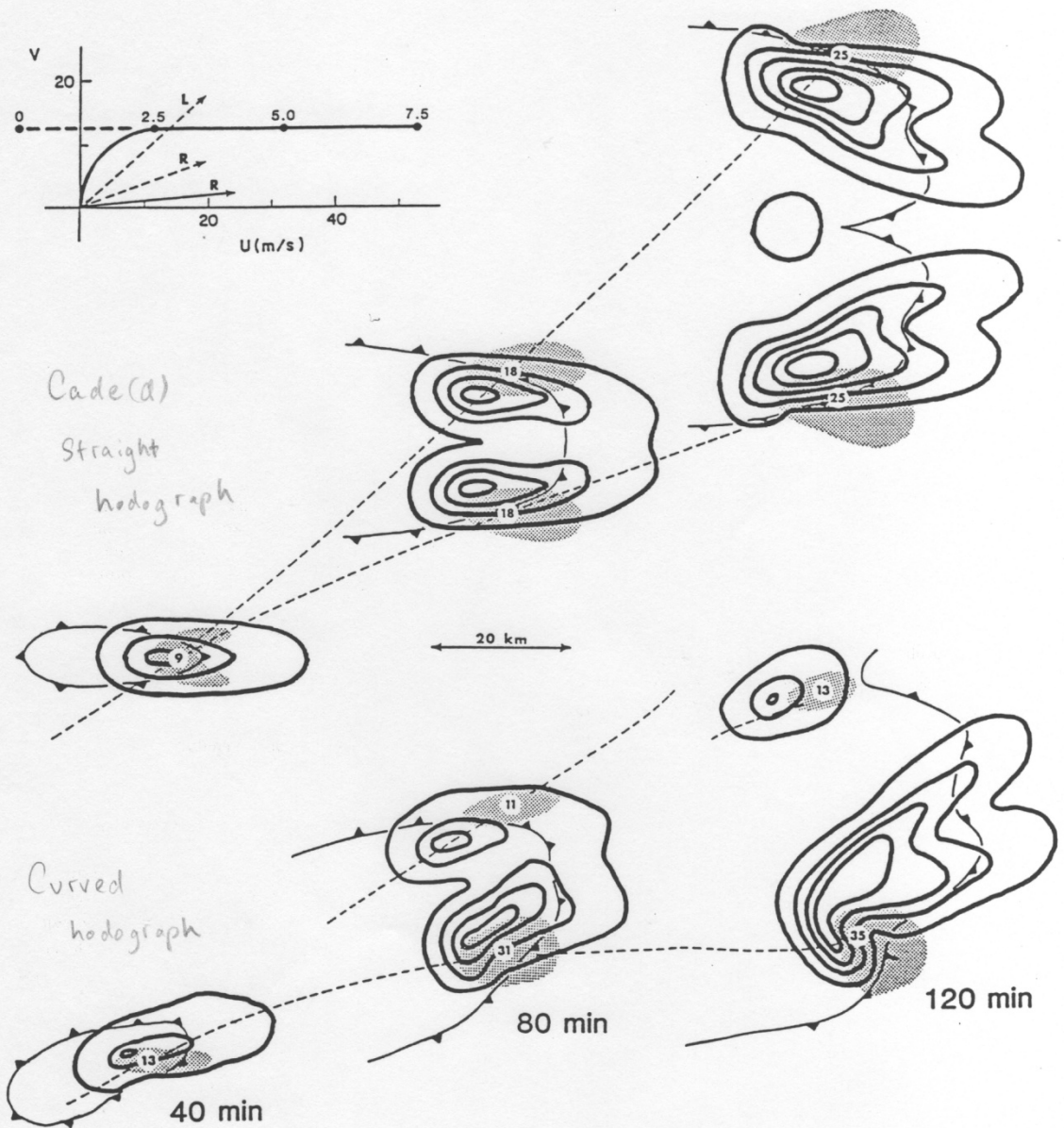
Same - but shear increased by 50% (f) $R=20$

CASE F



CASE D

*Unidirectional shear
No helicity*

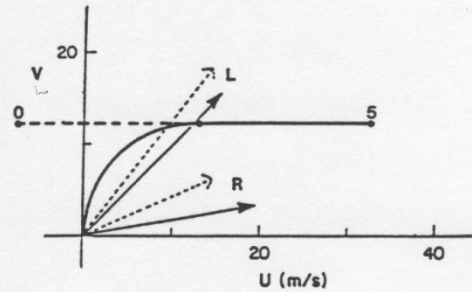


CASE D

*Directional shear
Has helicity*

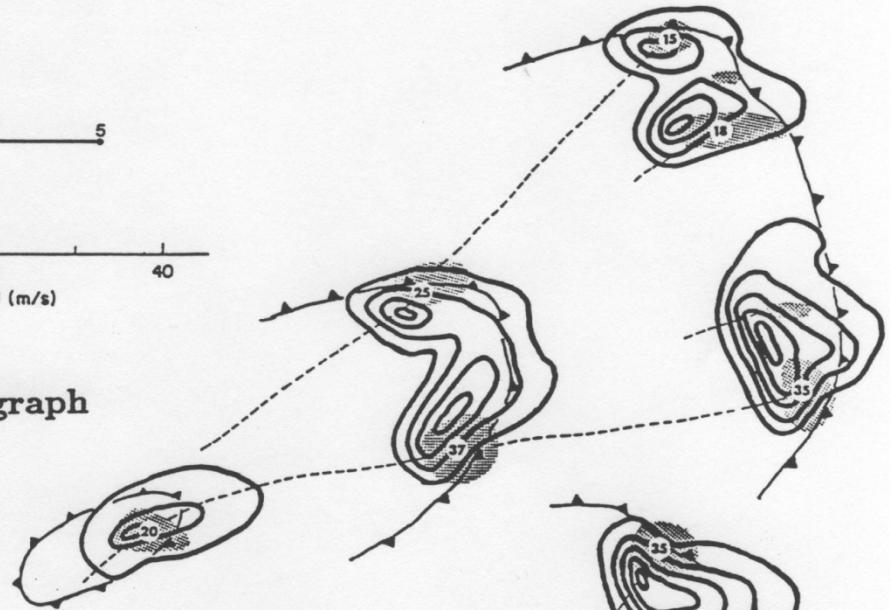
CASE C

Directional shear
Has helicity



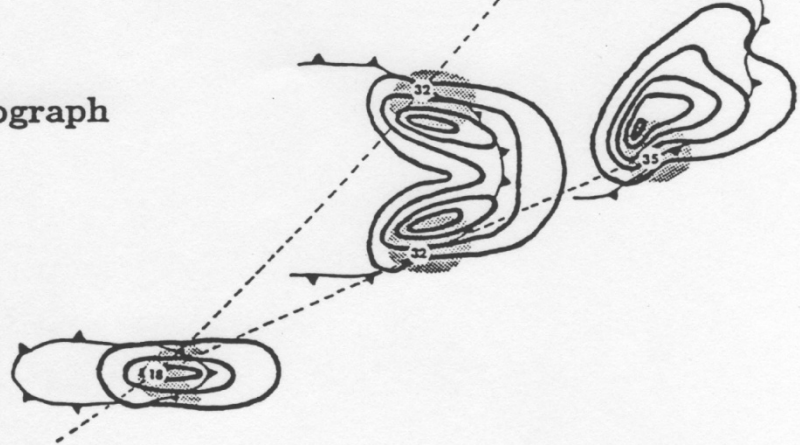
Curved Hodograph

$R = 15$



Straight Hodograph

$R = 12$



CASE C

Unidirectional shear
No helicity